



UNIL | Université de Lausanne

Unicentre

CH-1015 Lausanne

<http://serval.unil.ch>

Year : 2020

Glial cells of the human fovea

Khamsy Lilly

Khamsy Lilly, 2020, Glial cells of the human fovea

Originally published at : Thesis, University of Lausanne

Posted at the University of Lausanne Open Archive <http://serval.unil.ch>

Document URN : urn:nbn:ch:serval-BIB_D568B5CD13A13

Droits d'auteur

L'Université de Lausanne attire expressément l'attention des utilisateurs sur le fait que tous les documents publiés dans l'Archive SERVAL sont protégés par le droit d'auteur, conformément à la loi fédérale sur le droit d'auteur et les droits voisins (LDA). A ce titre, il est indispensable d'obtenir le consentement préalable de l'auteur et/ou de l'éditeur avant toute utilisation d'une oeuvre ou d'une partie d'une oeuvre ne relevant pas d'une utilisation à des fins personnelles au sens de la LDA (art. 19, al. 1 lettre a). A défaut, tout contrevenant s'expose aux sanctions prévues par cette loi. Nous déclinons toute responsabilité en la matière.

Copyright

The University of Lausanne expressly draws the attention of users to the fact that all documents published in the SERVAL Archive are protected by copyright in accordance with federal law on copyright and similar rights (LDA). Accordingly it is indispensable to obtain prior consent from the author and/or publisher before any use of a work or part of a work for purposes other than personal use within the meaning of LDA (art. 19, para. 1 letter a). Failure to do so will expose offenders to the sanctions laid down by this law. We accept no liability in this respect.



UNIL | Université de Lausanne

Faculté de biologie
et de médecine

UNIVERSITE DE LAUSANNE - FACULTE DE BIOLOGIE ET DE MEDECINE

Département universitaire d'Ophtalmologie

Service de recherche translationnelle

Glial cells of the human fovea

THESE

préparée sous la direction de Professeure Francine Behar-Cohen

et présentée à la Faculté de biologie et de médecine de
l'Université de Lausanne pour l'obtention du grade de

DOCTEUR EN MEDECINE

par

Lilly KHAMSY

Médecin diplômée de la Confédération Suisse
Originaire de Berne

Lausanne
2020



UNIL | Université de Lausanne

Faculté de biologie
et de médecine

UNIVERSITE DE LAUSANNE - FACULTE DE BIOLOGIE ET DE MEDECINE

Département universitaire d'Ophtalmologie

Service de recherche translationnelle

Glial cells of the human fovea

THESE

préparée sous la direction de Professeure Francine Behar-Cohen

et présentée à la Faculté de biologie et de médecine de
l'Université de Lausanne pour l'obtention du grade de

DOCTEUR EN MEDECINE

par

Lilly KHAMSY

Médecin diplômée de la Confédération Suisse
Originaire de Berne

Lausanne
2020

Imprimatur

Vu le rapport présenté par le jury d'examen, composé de

Directeur de thèse *Madame la Professeure **Francine Behar-Cohen***

Co-Directeur de thèse

Expert

**Vice-Directeur de
l'Ecole doctorale** *Monsieur le Professeur **John Prior***

la Commission MD de l'Ecole doctorale autorise l'impression de la thèse de

Madame Lilly KHAMSY

intitulée

Glial cells of the human fovea

Lausanne, le 19 mai 2020

*pour Le Doyen
de la Faculté de Biologie et de Médecine*



*Monsieur le Professeur John Prior
Vice-Directeur de l'Ecole doctorale*

Résumé

Thèse de doctorat en médecine de Lilly Khamsy
préparée sous la direction de Professeure Francine Behar-Cohen

Contexte du travail de recherche

Ce travail de thèse a débuté dans le cadre d'un MD PhD en décembre 2015 au sein du laboratoire de recherche fondamentale de l'Hôpital Jules Gonin à Lausanne sous la direction de Professeure Behar-Cohen. Suite aux changements à la Direction de l'Hôpital Jules Gonin ce travail de thèse s'est transformé en MD en mai 2017.

Enjeux de la recherche

Le but du projet de recherche MD PhD est d'étudier l'homéostasie de la rétine, en particulier l'influence de l'insuline sur les échanges hydrostatiques et électrolytiques des cellules de l'épithélium pigmentaire de la rétine (RPE). En effet, il a été suggéré par des observations cliniques (Gubitosi-Klug RA et al. 2016, Zhang J et al. 2015, Klefter ON et al. 2016) et des données expérimentales (Sugimoto M et al. 2013) que les taux élevés d'insuline chez les patients diabétiques de type 2 insulino-résistants altèrent les jonctions serrées des RPE et conduisent à une péjoration de l'acuité visuelle. Le projet de MD s'est concentré sur l'architecture de la macula humaine, plus particulièrement de la fovea, où les altérations d'homéostasie peuvent conduire au développement d'œdèmes maculaires chez les patients diabétiques.

Méthodes et Résultats

Les travaux préliminaires ont porté sur une lignée cellulaire de RPE (ARPE19) exposée à des concentrations variables de glucose et d'insuline. Les marquages des jonctions cellulaires (Zona occludens-1) suggèrent que les cellules exposées à une forte concentration de glucose ouvrent leurs jonctions en présence d'insuline (Annexe 1, rapport de 1^{ère} année de MD PhD).

Afin de vérifier ces observations dans un autre modèle, des cellules souches pluripotentes (human Induced Pluripotent Stem cells, hIPS) ont été induites en RPE dans les laboratoires de l'Hôpital Jules Gonin. Or, le milieu utilisé pour cultiver les cellules hIPS-RPE contient des niveaux importants d'insuline dans le supplément de culture B27. Une étude de privation a pu établir que les hIPS-RPE peuvent survivre en maintenant leurs caractéristiques de différenciation en absence de ce supplément riche en insuline (Annexe 2, manuscrit 01.2020).

Les travaux *in vivo* ont porté sur un modèle de rat diabétique de type 2, le rat Goto-Kakizaki. Afin d'éviter l'hypoglycémie induite par l'injection systémique d'insuline, nous avons effectué des injections d'insuline intravitréales (dans le corps vitré). La glycémie de ces animaux n'a pas été influencée par ces injections. Nous avons observé la dilatation des vaisseaux au fond d'œil ainsi que des fuites de produit de contraste à l'angiographie au FITC dextran dans les conditions diabétiques lors de l'application d'insuline. Ces résultats suggèrent une influence de l'insuline sur la perméabilité des vaisseaux de la rétine (Annexe 3, présentation au congrès ARVO 2017).

Enfin une collection de globes humains composée de globes oculaires de patients énucléés pour tumeur intraoculaire ainsi que de globes oculaires de donneurs sains *post mortem* a été constituée. Ces spécimens ont servis à effectuer le marquage immunohistochimique des cellules qui composent la fovea. Nous avons pu démontrer grâce à ces marquages la présence de cellules gliales astrocytaires dans la fovea humaine. Les résultats de cette étude font l'objet de la publication soumis pour ce travail de doctorat (Annexe 4, publication Molecular Vision).

Conclusion

Les travaux préliminaires *in vitro* et *in vivo* ont permis d'établir une potentielle influence de l'insuline sur les cellules et vaisseaux de la rétine. La reproduction de ces résultats serait nécessaire pour valider ces observations. Les travaux sur les tissus humains, ont permis de démontrer la présence de cellules gliales astrocytaires dans la fovea humaine, ce qui est un résultat important. Leurs rôles dans l'homéostasie de la macula et les pathologies maculaires restent à être déterminés. Cette découverte permet d'interpréter les images cliniques en prenant en compte cette nouvelle entité cellulaire.



UNIL | Université de Lausanne

Faculté de biologie
et de médecine

Annexes

Thèse de doctorat en médecine de Lilly Khamsy
préparée sous la direction de Professeure Francine Behar-Cohen

Annexe 1 : rapport de 1^{ère} année de MD PhD

The influence of glycemic-controlling drugs on retinal homeostasis: Evaluation of insulin and Glucagon-like-peptide 1 role on hydro-electrolytic retinal homeostasis

MD-PhD candidate: Lilly Khamsy, medical doctor

Thesis director: Pr Francine Behar-Cohen, Department of ophthalmology, University of Lausanne.

15/05/16
Prof. F. Behar-Cohen
Cheffe de service

Background

To date, 382 million persons suffer from diabetes mellitus type II and, due to the worldwide increasing obesity and sedentary lifestyle, diabetes prevalence is expected to double within the next 20 years (1, 2). Amongst diabetic complications, diabetic macular edema (DME) is the main cause of vision loss, affecting working-age individuals, impairing their independence and life quality (3, 4). The current understanding of the pathogenesis leading to DME is chronic hyperglycemia inducing retinal microangiopathy with subsequent breakdown of the blood retinal barriers (5, 6). The retinal pigment epithelium (RPE) monolayer seals the retina by forming tight junctions preventing diffusion of solutes across the paracellular space, establishing and maintaining a concentration gradient between apical and basal environments. Numerous clinical studies describe temporary paradoxical worsening of diabetic macular edema after insulin treatment independent of glycemic control (7-11). Although metabolic control is crucial for maintenance of cell homeostasis and barrier function, accumulating clinical (12-15) and experimental data (9) suggest high level of insulin being involved in diabetes-mediated RPE damage leading to tight junction breakdown. Hyperglycemia and reactive oxygen species levels increase RhoA/Rho-kinase (ROCK) activity (16), a GTPase modulating cytoskeleton contractility, cell polarization and cell-cell junction (17, 18) suggesting its involvement in tight junction rearrangement preceding barrier breakdown. In the RPE, functional insulin receptors have been identified (19-21), and studies suggests that insulin signaling cascade might modulate ROKalpha through insulin receptor substrate-1 (22, 23). It has been shown that an inhibitor of RhoA protein kinase, Glucagon-like peptide-1 (GLP-1) a glycemia controlling drug (24, 25) reduces retinal leakage in type II diabetic rats and in vitro (26-28). Our working hypothesis is that insulin in oxidative conditions modulates cortical actin cytoskeleton rearrangement in the retinal pigment epithelium through RhoKinase leading to alteration of tight junctions. We hypothesize that GLP-1 through moderate RhoKinase inhibition, might reverse its over activation thus restoring retinal barriers.

Introduction

We started by performing a set of experiments using ARPE19 cell line exposing them to various concentrations of glucose and insulin. This spontaneous RPE cell line derives from the globe of a 19-year old male donor from Lions Eye and Tissue Bank, Sacramento, CA, U.S.A in 1996 (29). The choice of glucose concentration was made according to previous literature (30, 31) and the choice of insulin concentration was made according to activation of the PI3K/Akt/PKB and the MAPK insulin signaling pathway (32, 33). The aim of this study was to explore the effect of glucose and insulin on the permeability (transepithelial resistance) and distribution of tight junctions (ZO-1) in a human RPE cell line.

Material and Methods

Human RPE cell culture

Retinal pigment epithelium cell lines of human origin (ARPE19) were obtained from the host lab at passage 16. The cells were expanded successively in T5, T25, T75 flasks following Dunn et al. protocol (29) in a medium with DMEM (Dulbecco's modified Eagle, Cat. No. 32430-027, LifeTech) containing 4.5g/l Glucose (25mM) supplemented with 10% fetal bovine serum (FBS, F7524, Sigma-Aldrich), 1% penicillin-streptomycin (Sigma Aldrich) and 1% sulfate pyruvate (S8636, Sigma Aldrich). Cells were then plated on 12-well plastic transwells (diameter 1.12cm², polyester filters; CLS3460-48EA, HTS-Transwell, Costar; Corning Inc, NY, USA). After reaching 80-90% confluence (48h), FBS concentration was reduced to 1% for 48 days ± 5 days before treatment. Cells were starved from FBS 24h before experiments and during the treatment period. Cells were incubated at 37°C in 5% CO₂. Medium was changed every 3 days.

Cells were exposed seven days to various glucose (Sigma Aldrich) (25mM, 40mM) and insulin (insulin recombinant human, 91077C Sigma Aldrich) concentration (0, 10, 100nM). D-Mannose (M6020, Sigma Aldrich) was used as an osmotic control agent (25mM Glucose + 15mM Mannose vs 40mM Glucose). In a second set of experiment glucose concentration was raised from 5mM to 25mM, D-Mannose (5.5mM Glucose + 21.5mM Mannose). After 3 days treatment the medium was changed.

Measurement of TER

Transepithelial resistance (TER) was measured using an epithelial voltmeter (EVOM2, World Precision Instruments, Sarasota, FL, USA). TER measurements were performed under the hood, within 3 min of removal from the incubator, average temperature is 32.2 ± 1.85°C. Net TER calculated were calculated by subtracting the resistance of the transwell filter without cells from the values obtained with the filters with ARPE19 cells, and multiplied with the effective growth area. Measurements were performed every day, 3 times per well with 10 minutes interval allowing temperature stabilization in the incubator.

Immunofluorescence staining

Immunofluorescence was performed after the 7 days treatment. Cells on transwell were fixed with 4% Paraformaldehyde for 30min, washed once with PBS and blocked with PBS 10% FBS 0.1% TritonX100 for 30min at 37°C. Rabbit anti-ZO-1 (1:250) were incubated overnight (16-18h). After washing 3x in blocking buffer, incubation with Goat anti-rabbit secondary antibody (1:300) for 1h at room temperature. See Table 1. After washing 3x in blocking buffer and 5min DAPI staining, transwell filters were mounted with Mowiol. Images were acquired with an Olympus DP72 an upright fluorescence microscope.

Results

Our preliminary data consistently show opened tight junctions in high glucose (Glucose 40mM) and 10nM insulin concentration compared with normal glucose and insulin conditions were ARPE19 cells exhibit intact *cobblestone* appearance (Fig. 1). These preliminary findings reveal that insulin in combination of high glucose impairs tight junctions. Additionally we observed that hyperosmolarity increases transepithelial resistance in accordance with other publications (34, 35) conducted in high NaCl condition.

Perspectives

We will study expression and distribution of tight junction proteins, RhoK and phosphorylated occludin in further experiments using following models:

hiPSc RPE model

We will use Human induced pluripotent stem cells derived RPE generated following an adapted version of the protocol of Gamm et al. (36). These cells express a closer phenotype to human in vivo RPE cells. However their cultivating medium contains B27 (125870-01, Life Technologies) supplement which contains high concentration of insulin. B27 starving experiments are ongoing.

Goto-Kakizaki rat model

We started breeding a spontaneous type II diabetic rat model starting with 3 males and 3 females, we obtained 27 F1 males and 43 F1 females. Glycemia values of >12mmol/L were obtained from all males at 3 months of age, and as according to the literature females maintained normoglycemic phenotype (37)

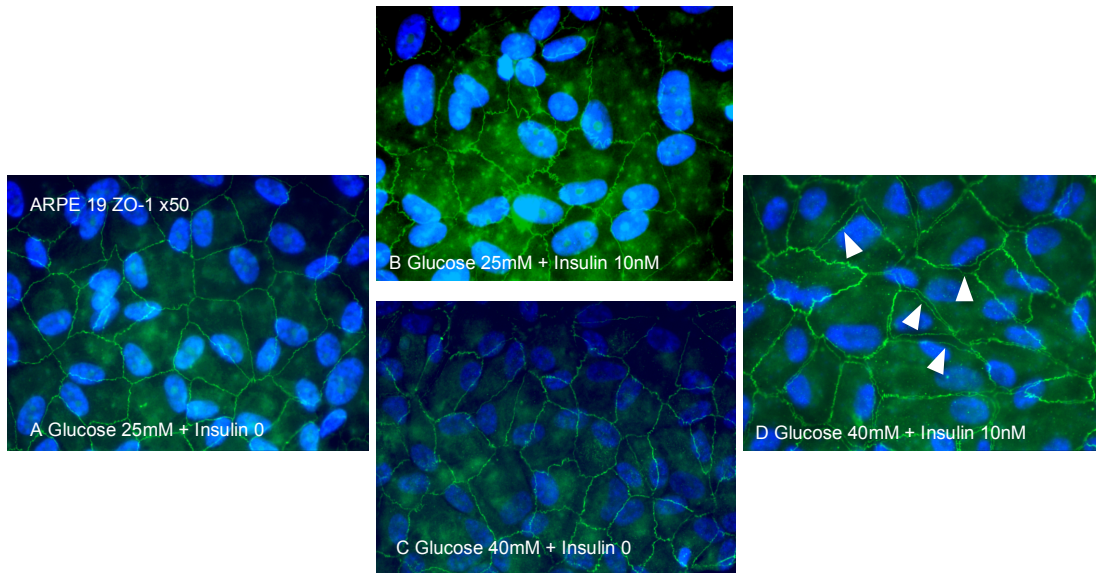


Fig. 1 ARPE19 ZO-1 staining. ZO-1 associated Tight Junction protein, anchors occluding to actin cytoskeleton. (A) Regular cobblestone staining pattern in baseline conditions. (B) Stressed pattern in presence of 10nM of insulin and (C) exposed to high glucose without insulin. (D) In presence of combination of high glucose and insulin 10nM increased spacing is observed between the cells.

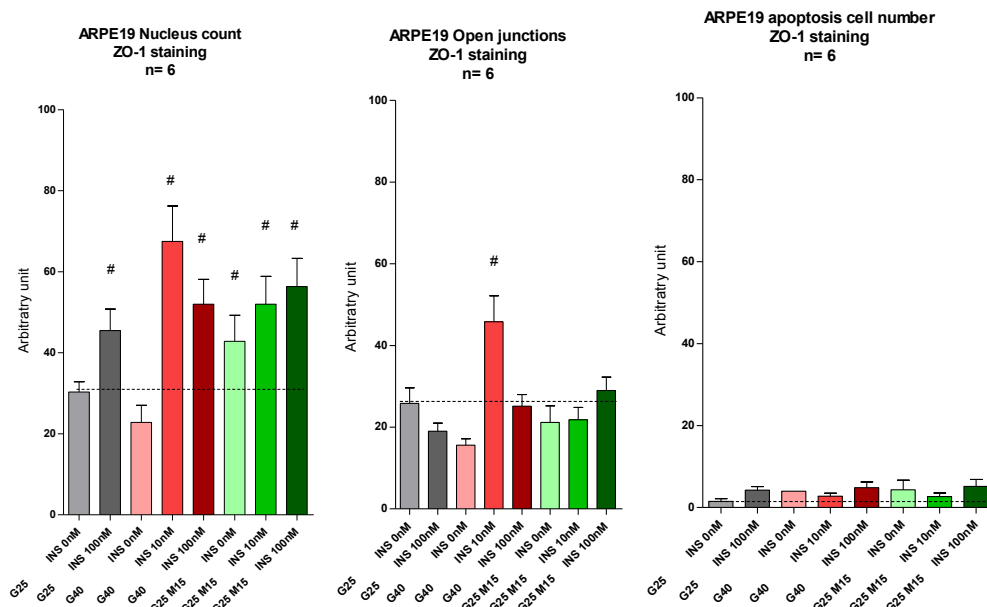


Fig. 2 Results of ARPE19 quantification of nucleus, open junctions and apoptotic cells from ZO-1 Immunofluorescence staining. Bars represent the mean \pm SD of 6 pictures X20 taken from 6 wells (n=6). Of note, exclusion of ZO-1 staining of Glucose 25mM Insulin 10nM condition because of bleaching. Dotted line represents baseline condition. Levels of statistical significance were set at $p < 0.05$

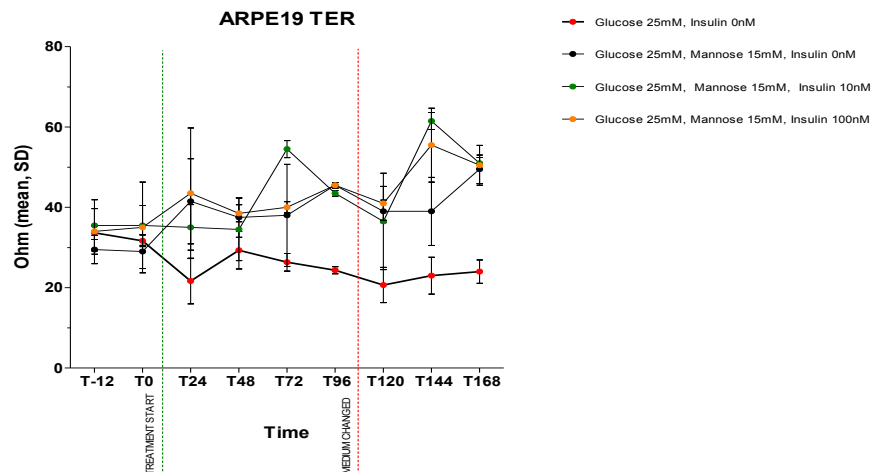


Fig 3. Results of TER. The vertical axis represents the TER, expressed in $\text{Ohm} \times \text{cm}^2$ and the horizontal axis the time. The medium was replaced with fresh medium after 3 days. Each point represents the mean of 3 measurements on 3 different well treated with the same condition (n=3). Bars represent SD.

1. Antibodies references for immunofluorescence staining

ZO-1	Zona Occludens prot. 1 (N-term.)	40-2300	Zymed
Phalloidin	Rhodamine conjugated	R415	Life Technologies
Goat Anti-Rabbi IgG	Alexa Fluor 488nm	150077	Abcam

- Group IDFDA. Update of mortality attributable to diabetes for the IDF Diabetes Atlas: Estimates for the year 2013. *Diabetes Res Clin Pract.* 2015;109(3):461-5.
- Guariguata L, Whiting DR, Hambleton I, Beagley J, Linnenkamp U, Shaw JE. Global estimates of diabetes prevalence for 2013 and projections for 2035. *Diabetes Res Clin Pract.* 2014;103(2):137-49.
- Varma R, Bressler NM, Doan QV, Gleeson M, Danese M, Bower JK, et al. Prevalence of and risk factors for diabetic macular edema in the United States. *JAMA Ophthalmol.* 2014;132(11):1334-40.
- Bourne RR, Jonas JB, Flaxman SR, Keeffe J, Leasher J, Naidoo K, et al. Prevalence and causes of vision loss in high-income countries and in Eastern and Central Europe: 1990-2010. *Br J Ophthalmol.* 2014;98(5):629-38.
- Klaassen I, Van Noorden CJ, Schlingemann RO. Molecular basis of the inner blood-retinal barrier and its breakdown in diabetic macular edema and other pathological conditions. *Prog Retin Eye Res.* 2013;34:19-48.
- Omri S, Behar-Cohen F, de Kozak Y, Sennlaub F, Verissimo LM, Jonet L, et al. Microglia/macrophages migrate through retinal epithelium barrier by a transcellular route in diabetic retinopathy: role of PKCzeta in the Goto Kakizaki rat model. *Am J Pathol.* 2011;179(2):942-53.
- Henricsson M, Janzon L, Groop L. Progression of retinopathy after change of treatment from oral antihyperglycemic agents to insulin in patients with NIDDM. *Diabetes Care.* 1995;18(12):1571-6.
- Wu H, Xu G, Liao Y, Ren H, Fan J, Sun Z, et al. Supplementation with antioxidants attenuates transient worsening of retinopathy in diabetes caused by acute intensive insulin therapy. *Graefes Arch Clin Exp Ophthalmol.* 2012;250(10):1453-8.
- Sugimoto M, Cutler A, Shen B, Moss SE, Iyengar SK, Klein R, et al. Inhibition of EGF signaling protects the diabetic retina from insulin-induced vascular leakage. *Am J Pathol.* 2013;183(3):987-95.
- Agardh CD, Eckert B, Agardh E. Irreversible progression of severe retinopathy in young type I insulin-dependent diabetes mellitus patients after improved metabolic control. *J Diabetes Complications.* 1992;6(2):96-100.
- Moskalets E, Galstyan G, Starostina E, Antsiferov M, Chantelau E. Association of blindness to intensification of glycemic control in insulin-dependent diabetes mellitus. *J Diabetes Complications.* 1994;8(1):45-50.
- Writing Team for the DERG, Gubitosi-Klug RA, Sun W, Cleary PA, Braffett BH, Aiello LP, et al. Effects of Prior Intensive Insulin Therapy and Risk Factors on Patient-Reported Visual Function Outcomes in the Diabetes Control and Complications Trial/Epidemiology of Diabetes Interventions and Complications (DCCT/EDIC) Cohort. *JAMA Ophthalmol.* 2016;134(2):137-45.
- Zhang J, Ma J, Zhou N, Zhang B, An J. Insulin use and risk of diabetic macular edema in diabetes mellitus: a systemic review and meta-analysis of observational studies. *Med Sci Monit.* 2015;21:929-36.
- Klefter ON, Hommel E, Munch IC, Norgaard K, Madsbad S, Larsen M. Retinal characteristics during 1 year of insulin pump therapy in type 1 diabetes: a prospective, controlled, observational study. *Acta Ophthalmol.* 2016.
- Zhang P, Liu N, Wang Y. Insulin may cause deterioration of proliferative diabetic retinopathy. *Med Hypotheses.* 2009;72(3):306-8.
- Leguina-Ruzzi A, Pereira J, Pereira-Flores K, Valderas JP, Mezzano D, Velarde V, et al. Increased RhoA/Rho-Kinase Activity and Markers of Endothelial Dysfunction in Young Adult Subjects with Metabolic Syndrome. *Metab Syndr Relat Disord.* 2015;13(9):373-80.
- Mason FM, Tworoger M, Martin AC. Apical domain polarization localizes actin-myosin activity to drive ratchet-like apical constriction. *Nat Cell Biol.* 2013;15(8):926-36.
- Citi S, Guerrero D, Spadaro D, Shah J. Epithelial junctions and Rho family GTPases: the zonular signalosome. *Small GTPases.* 2014;5(4):1-15.
- Naeser P. Insulin receptors in human ocular tissues. Immunohistochemical demonstration in normal and diabetic eyes. *Ups J Med Sci.* 1997;102(1):35-40.
- Ocrant I, Fay CT, Parmelee JT. Expression of insulin and insulin-like growth factor receptors and binding proteins by retinal pigment epithelium. *Exp Eye Res.* 1991;52(5):581-9.
- Thevis M, Thomas A, Schanzer W, Ostman P, Ojanpera I. Measuring insulin in human vitreous humour using LC-MS/MS. *Drug Test Anal.* 2012;4(1):53-6.
- Farah S, Agazie Y, Ohan N, Ngsee JK, Liu XJ. A rho-associated protein kinase, ROKalpha, binds insulin receptor substrate-1 and modulates insulin signaling. *J Biol Chem.* 1998;273(8):4740-6.
- Truebestein L, Elsner DJ, Fuchs E, Leonard TA. A molecular ruler regulates cytoskeletal remodelling by the Rho kinases. *Nat Commun.* 2015;6:10029.
- Kong X, Yan D, Sun J, Wu X, Mulder H, Hua X, et al. Glucagon-like peptide 1 stimulates insulin secretion via inhibiting RhoA/ROCK signaling and disassembling glucotoxicity-induced stress fibers. *Endocrinology.* 2014;155(12):4676-85.
- Tang ST, Zhang Q, Tang HQ, Wang CJ, Su H, Zhou Q, et al. Effects of glucagon-like peptide-1 on advanced glycation endproduct-induced aortic endothelial dysfunction in streptozotocin-induced diabetic rats: possible roles of Rho kinase- and AMP kinase-mediated nuclear factor kappaB signaling pathways. *Endocrine.* 2016;53(1):107-16.
- Fan Y, Liu K, Wang Q, Ruan Y, Ye W, Zhang Y. Exendin-4 alleviates retinal vascular leakage by protecting the blood-retinal barrier and reducing retinal vascular permeability in diabetic Goto-Kakizaki rats. *Exp Eye Res.* 2014;127:104-16.
- Fu Z, Kuang HY, Hao M, Gao XY, Liu Y, Shao N. Protection of exenatide for retinal ganglion cells with different glucose concentrations. *Peptides.* 2012;37(1):25-31.
- Hernandez C, Bogdanov P, Corraliza L, Garcia-Ramirez M, Sola-Adell C, Arranz JA, et al. Topical Administration of GLP-1 Receptor Agonists Prevents Retinal Neurodegeneration in Experimental Diabetes. *Diabetes.* 2016;65(1):172-87.
- Dunn KC, Aotaki-Keen AE, Putkey FR, Hjelmeland LM. ARPE-19, a human retinal pigment epithelial cell line with differentiated properties. *Exp Eye Res.* 1996;62(2):155-69.
- Hernandez C, Zapata MA, Losada E, Villarroel M, Garcia-Ramirez M, Garcia-Arumi J, et al. Effect of intensive insulin therapy on macular biometrics, plasma VEGF and its soluble receptor in newly diagnosed diabetic patients. *Diabetes Metab Res Rev.* 2010;26(5):386-92.
- Chen M, Wang W, Ma J, Ye P, Wang K. High glucose induces mitochondrial dysfunction and apoptosis in human retinal pigment epithelium cells via promoting SOCS1 and Fas/FasL signaling. *Cytokine.* 2016;78:94-102.
- Rodriguez A, Catalan V, Gomez-Ambrosi J, Garcia-Navarro S, Rotellar F, Valenti V, et al. Insulin- and leptin-mediated control of aquaglyceroporins in human adipocytes and hepatocytes is mediated via the PI3K/Akt/mTOR signaling cascade. *J Clin Endocrinol Metab.* 2011;96(4):E586-97.
- Taniguchi CM, Emanuelli B, Kahn CR. Critical nodes in signalling pathways: insights into insulin action. *Nat Rev Mol Cell Biol.* 2006;7(2):85-96.
- Willermain F, Libert S, Motulsky E, Salik D, Caspers L, Perret J, et al. Origins and consequences of hyperosmolar stress in retinal pigmented epithelial cells. *Front Physiol.* 2014;5:199.
- Wang H, Ferraris JD, Klein JD, Sands JM, Burg MB, Zhou X. PKC-alpha contributes to high NaCl-induced activation of NFAT5 (TonEBP/OREBP) through MAPK ERK1/2. *Am J Physiol Renal Physiol.* 2015;308(2):F140-8.
- Singh R, Phillips MJ, Kuai D, Meyer J, Martin JM, Smith MA, et al. Functional analysis of serially expanded human iPS cell-derived RPE cultures. *Invest Ophthalmol Vis Sci.* 2013;54(10):6767-78.
- Akash MS, Rehman K, Chen S. Goto-Kakizaki rats: its suitability as non-obese diabetic animal model for spontaneous type 2 diabetes mellitus. *Curr Diabetes Rev.* 2013;9(5):387-96.



UNIL | Université de Lausanne

Faculté de biologie
et de médecine

Annexes

Thèse de doctorat en médecine de Lilly Khamsy
préparée sous la direction de Professeure Francine Behar-Cohen

Annexe 2 : manuscript 01.2020

Title: Effect of B-27 Supplement starvation on human induced pluripotent stem cell-derived retinal pigment epithelium (hiPSC-RPE).

Original contribution**Article**

Title: Effect of B-27 Supplement starvation on human induced pluripotent stem cell-derived retinal pigment epithelium (hiPSC-RPE).

Title (2nd language): Effekt des B-27-Supplemententzugs auf retinales Pigmentepithel von humanen induzierten pluripotenten Stammzellen abgeleitet (hiPSC-RPE).

Authors

Lilly Khamsy^{1,2}
 Laura Kowalczyk^{1,3}
 Tatiana Favez³
 Sarah Decembrini⁴
 Florian Udry³
 Yvan Arsenijevic³
 Francine Behar-Cohen^{1,5}

Affiliation

¹ Faculty of Biology and Medicine, University of Lausanne, Lausanne, Switzerland

² Department of Ophthalmology, Inselspital, Bern University Hospital, University of Bern, Bern, Switzerland

³ Unit of Retinal Degeneration and Regeneration, Department of Ophthalmology, University of Lausanne, Jules-Gonin Eye Hospital, Fondation Asile des Aveugles, Lausanne, Switzerland.

⁴ Department of Physiology, Bern University Hospital, University of Bern, Bern, Switzerland

⁵ Centre de Recherche des Cordeliers UMRS1138, Team 17, INSERM, Paris, France

Corresponding address

Lilly Khamsy lillykhamsy@gmail.com

Abstract

Although preventing diabetic related complication, initiation of insulin therapy in type 2 diabetic patients potentially increases the risk of diabetic retinopathy and macular edema. However, the direct effect of insulin on the retinal pigment epithelium (RPE) remains incompletely understood. In order to develop a cell culture model suitable for testing insulin effects on RPE cells, insulin-free culture conditions are required. Yet the widely used B-27 Supplement for RPE cell culture contains high levels of insulin. We observed the cell characteristics after removal of B-27 Supplement in culture media for 7 days. We established a new B-27 free media able to maintain features of mature human induced pluripotent stem cell (hiPSC)-RPE cells such as morphology and markers of RPE differentiation. Moreover, we observed transepithelial resistance values closer to published native human RPE cells data. We concluded that B-27 Supplement-free culture condition is possible for testing insulin effects in hiPSC-RPE cell models.

Key words: Diabetic retinopathy, cell culture, insulin, retinal pigment epithelium, human induced pluripotent stem cell

Abstrakt (2nd language)

Insulintherapie verhindert Komplikationen im Zusammenhang mit Diabetes, jedoch die Einleitung einer Insulintherapie erhöht bei Typ-2-Diabetikern das Risiko einer diabetischen Retinopathie und eines Makulaödems. Die Auswirkungen von Insulin auf das retinales Pigmentepithel (RPE) ist jedoch unvollständig geklärt. Um ein Zellkulturmodell zu entwickeln, das zum Testen von Insulinwirkungen auf RPE-Zellen geeignet ist, sind insulinfreie Kulturbedingungen erforderlich. Das weitverbreitete B-27 Supplement für RPE-Zellkulturen enthält jedoch hohe Insulinkonzentrationen. Deshalb untersuchten wir die Zelleigenschaften von RPE-Zellen nach Entzug des B-27 Supplements in Medien während 7 Tagen. Die Zellmorphologie von RPE-Zellen welche aus humanen induzierten pluripotenten Stammzellen (hiPSC) entwickelt wurden, blieb nach Entzug des B-27 Supplements unverändert, wie auch die Expression von Markerproteine der RPE-Differenzierung. Die transepithelialen Resistenzwerte der hiPSC-RPE Zellen lagen auch näher den publizierten humanen RPE-Zellen Werten, wenn die RPE-Zellen ohne B27 Supplement kultiviert wurden. B-27 Supplement-freies Zellkulturmedium konnte also hiPSC-RPE-Zellen kultivieren um Auswirkungen von hinzugefügtem Insulin zu testen erlauben.

Keyword: Diabetische Retinopathie, Zellkulturemodell, Zellkultur, Insulin, retinales Pigmentepithel, humane induzierte pluripotente Stammzellen

Introduction

To date 425 million persons suffer worldwide from diabetes and, due to sedentary lifestyle and increasing incidence of obesity, the prevalence of diabetes is expected to double within the next 20 years¹. Among diabetic complications, diabetic macular edema (DME) is the main cause of vision loss affecting working age individuals, strongly impairing their daily life, independence and life quality^{2,3}. DME incidence reaches up to 25.4% of type 2 diabetic patients requiring insulin injections and 13.9% in those not requiring insulin^{4,5}. Chronic hyperglycemia induces retinal microangiopathy with subsequent breakdown of the blood retinal barrier leading to fluid accumulation in the macular region. This results in significant vision loss as macula mediates sharp focus and central vision. However, the exact mechanisms leading to DME formation remain poorly understood, limiting new therapeutic options. The drugs commonly used to control glucose blood levels (i.e. insulin, GLP-1 analogues) seem to influence DME pathophysiology^{6,7}. Initiation of acute intensive insulin therapy in patients with long-standing poor glycemic control results in worsening of diabetic retinopathy⁸. Furthermore, a change in treatment from oral drugs to subcutaneous insulin in type 2 diabetes patients is associated with a significant risk of retinopathy progression and visual impairment^{9,10}. Of particular interest is the retinal pigment epithelial (RPE), a single layer of epithelial cells between the retina and the choroid playing, a key role in the maintenance of photoreceptor cells responsible for capturing light and transmitting inputs to the superior cortical stations through the optic nerve. RPE cells form the outer blood retinal barrier through tight junctions and maintain the retina attached to the choroid by active outflow from the retina towards the choroid through ion and water channels (ENaC, NaK ATPase, chlorides channels, aquaporins...) ^{11,12,13}. Interestingly, studies show that insulin acts on ion and water channel expression in the kidney^{14,15} and in the placenta¹⁶, but the exact role of insulin on RPE ion and water channels and its subsequent role in fluid accumulation in the retina leading to DME formation has not been fully studied to date.

Induced pluripotent stem (iPSC) cells were initially established from mouse and subsequently from human cells by Takahashi and Yamanaka (2006,2007) ^{17,18} demonstrating successfully the reprogramming of human somatic cells into pluripotent cells. Since then, different protocols were established to derive human iPSC into RPE cells, generating a great in vitro model for ophthalmologic research. We derived RPE cells from hiPSC in order to conduct a systematic analysis of the effects of insulin on the retinal barriers and the hydro-electrolytic mechanisms. For this purpose, we required an insulin-free cell culture model. Yet the widely used B-27 Supplement for RPE cell culture maintenance contains high levels of insulin. B-27 Supplement in neuronal cultures supports cell growth¹⁹. It is a synthetic formulation that eliminates the need for supplementation with animal sera as a source for amino acids, proteins, vitamins, hormones, growth factors, minerals, lipids and other important micronutrients, thereby reduces variability of cell culture conditions^{20,21}. In this study, our purpose was to observe the feasibility of B-27 Supplement starvation in a cell culture model of human induced pluripotent stem cell derived-RPE cells.

Methods

1. Generation of hiPSC-RPE from hiPSC

hiPSC were kindly given to us from the laboratory of Pr. David Gamm, University of Wisconsin, USA. hiPSC were induced from dermal fibroblasts from healthy individuals according to the protocol described by Okita et al.²² We cultured hiPSC to obtain hiPSC-RPE using a protocol adapted from Sanoda et al.²³. Briefly, under feeder free conditions, hiPSC were cultured in mTeSR media kit (Cat.No. 5851 & 5852, StemCell) on Matrigel Embryonic Stem Cell Grade (Cat.No 354277, Corning). After reaching 60-80% confluence cells were lifted from the plate using a solution of type IV Collagenase (1ml/well of 6 well-plate, Cat.No. 17104-019, Life Technologies) at 400U/ml concentration in DMEM/F12 (Cat.No. 11330-032, LifeTechnologies). iPSC clumps are transferred into T25 flasks in 10ml Embryoid Body Media (EBM, DMEM/F12 (Cat.No. 11330-032, LifeTechnologies), 1% N2-100X Supplementation (Cat.No. 17502-048, LifeTechnologies), 1% B27-50X supplementation (Cat.No. 17504-044, LifeTechnologies), 1% L-glutamine (Cat.No. 25030-024, LifeTechnologies), 0.1mM Beta-Mercaptoethanol (Cat.No. M7522, Sigma Aldrich). On day 2, Embryoid-like bodies are plated on Matrigel Reduced Factor (MRF; dilution 1:30, Cat.No. 354230, Corning) coated plated in 6cm diameter petri dish at a density of 20-25 EBs*cm⁻². On day 4 and 7 media was changed to DMEM/F12 (Cat.No. 11330-032, LifeTechnologies), 1% N2-100X supplementation (Cat.No. 17502-048, LifeTechnologies), 1% L-glutamine (Cat.No. 25030-024, LifeTechnologies), 1% MEM-NEAA (Cat.No. 11140-035, LifeTechnologies), 2µg/ml Heparin (Cat.No. 375095-100KU, Millipore). On day 10 media was changed to Retinal Differentiation Media with vitamin A ; DMEM-Glutamax (Cat.No. 32430-027, Life Technologies) and F12 Nutrient Ham (Cat.No.21765-029, LifeTechnologies) in 3:1 proportion with 2% B-27 50X with vitamin A (Cat.No. 17504-044, LifeTechnologies). For pigmentation, media was changed on day 13 to Retinal Differentiation Media without vitamin A ; DMEM-Glutamax (Cat.No. 32430-027, Life Technologies) and F12 Nutrient Ham (Cat.No.21765-029, LifeTechnologies) in 3:1 proportion with 2% B-27 50X without vitamin A (Cat.No. 12587-010, LifeTechnologies). Pigmentation foci (PF) appearing around day 16-20 were collected manually in a polypropylene tube and plated directly on MRF in 2.5-4ml Retinal Differentiation Media with vitamin A for PF culture in 6cm diameter petri dish (1 to 3 PF/cm²). Media was changed once a week and after 30 days pigmented patches were collected and plated on MRF-coated plates at a density of 0.5 to 1.0x10⁵ cells/cm², cells were then considered to be at passage 1. After 30 days

cells were passaged and expanded on MRF-coated plate (1:30). For assay the iPSC-RPE were plated on MRF-coated 12-transwell (12 mm diameter, 0.4µm pore polyester membrane insert, CLS3460, Corning).

2. B-27 Supplement Composition

B-27 Supplement minus Vitamin A (Cat.No. 12587-010, LifeTechnologies) contains Biotin, Carnitine, D-Galactose, Putrescine, Selenium, Corticosterone, Linoleic acid, Linolenic acid, Progesterone, Retinyl acetate, D-1-alpha-Tocopherol, Bovine serum albumin, Catalase, Glutathione, Insulin, Superoxide dismutase,

Transferrin, Triodo-L-thyronine, the exact formulation is under industrial secret¹⁹. According to published data (Hanna, 2016; Bottenstein, 1979) the insulin concentration in B-27 Supplement amounts to 3-5 micrograms per ml^{24,25}.

3. B-27 Supplement Starvation Medium

At week 8 of culture passage 3 hiPSC-RPE cells the basal and apical medium 16 MRF-coated transwells was changed. Half of the transwell were filled with Retinal Differentiation Media without vitamin A (RDM) with DMEM-Glutamax (Cat.No. 32430-027, Life Technologies) and F12 Nutrient Ham (Cat.No. 21765-029, LifeTechnologies) in 3:1 proportion with 2% B-27 50X without vitamin A (Cat.No. 12587-010, LifeTechnologies). The other 8 transwells were filled with B-27 Starved Media (SM) with DMEM-Glutamax (Cat.No. 32430-027, Life Technologies) and F12 Nutrient Ham (Cat.No. 21765-029, LifeTechnologies) in 3:1 proportion.

4. Morphological characterization using light microscopy

hiPSC-RPE cells on 6-transwell plates were observed under an Olympus BX41 light microscope and 3 pictures per transwell in magnification 20X were taken on experimental day 0, 1, 5 and 7 after B-27-Supplement starvation. The images were split into 6 fields, total number of cells and pigmented cells per field were quantified manually on Fiji software. Results are expressed in percentage of pigmented cells per field. The pigmentation threshold of all the images used for cell counting was homogenized at 2-bits saturation.

5. Transepithelial resistance (TER)

Using manual chopstick electrode (World Precision Instruments, Sarasota, FL, USA) hiPSC-RPE monolayers cultured on transwell inserts in 12-well plates were measured daily. The chopstick electrodes were sterilized in 70% ethanol and since TER fluctuates with temperature, the electrodes were rinsed in SM at 37°C to allow temperature equilibration. The measurements were made within 3 min of removal of transwells from the incubator. For measurements, the shorter end of the chopstick electrode was placed in the upper chamber while the longer end was placed in the bottom chamber of the well, the chopstick was held in position until a TER reading was obtained. All TER-measurements were recorded in biological triplicate; the plates were placed in the incubator at least for 5 minutes between each measurement round. Net TER was calculated from average TER triplicate recordings by subtracting background resistance obtained from a negative control well, an MRF-coated insert with SM media without cells, subsequent value were multiplied by the surface area of the transwell filter (1.12cm²) and reported as Ω·cm². The negative control transwell without cells was treated similarly in regard of medium change.

6. hiPSC-RPE characterization

Cells were stained with RPE specific cell makers for immunostaining. Briefly, hiPSC-RPE were fixed with 4% paraformaldehyde for 15 minutes and washed twice with phosphate buffer saline (PBS). The transwell filters were carefully detached from the inserts using a sterile scalpel blade No 11 and disposed in 12-well plates containing a solution of 1xPBS, 10% Fetal Bovine Serum (Sigma) for 45 minutes to block non-specific binding sites. Permeabilization was performed using a solution containing 1xPBS, 0,3% Triton X-100 (Sigma) and 5% normal goat serum (Sigma) for one hour. Cells were incubated overnight at 4°C with the following primary antibodies diluted in blocking solution: RPE65 (1:200, AP07/2002), Bestrophin-1 (1:200, NB 300-164, Novus Biological, Littelton, CO, USA), cellular retinaldehyde-binding protein CRALBP (1:200, Ab 15051, Abcam, Cambridge, UK), zona occludens protein 1 ZO-1 (1:250, 40-220, Invitrogen). Cells were washed three times in PBS, and stained with the secondary antibodies 1:2000 in PBS with 1% BSA, 0.3% Triton X-100 (for RPE65, ZO-1 : Goat anti-rabbit IgG Alexa Fluor 488 (Abcam); for BEST-1 and CRALBP : Goat anti-mouse IgG Alexa Fluor 488 (Abcam)). Nuclei were stained with DAPI (1:10000, Invitrogen), washed three times in PBS and slides were mounted with Moviol (Sigma) and visualized with an Olympus BX60 fluorescence microscope at identical exposure and gain for all observed sections.

Statistical Analysis

All results were expressed as means ± SEM of the indicated number of experiments. Statistical analyses (one-way ANOVA) were performed with Prism 4.0.2 (GraphPad Software Inc., La Jolla, CA) and significance was reported for values p≤0.05.

Results

Our RPE differentiation protocol was adapted from Sanoda et al.²²³. Human iPSCs were expanded in T25 flasks and differentiated on coated 6cm dishes. Pigmented foci appeared around day 16-20 and were manually collected 30 days later. The pigmented foci harbor cells with typical RPE cobblestone morphology. After 30 days of expansion, the pigmented patches were dissected, dissociated and plated. After this step the cells were considered to be at passage 1 (P1). Once the RPE cells reach confluence (after 10 to 15 days), cell were passed for expansion on MRF-coated plates. For the assays RPE cells were then passaged on MRF-coated 12mm diameter transwell.

All assays performed were on P3 hiPS-RPE matured 8 weeks on transwell to allow time for the cells to reacquire RPE characteristics lost during the passages. Transwell culture system allows cells a polarized cell growth. The permeable membrane generate two compartments for the RPE monolayer, the apical (upper) compartment corresponds to the retinal facing side and the basolateral (lower) compartment corresponds to the choroidal facing side (Suppl. Fig.1).

B-27 Supplement starvation did not cause changes in hiPSC-RPE cell morphology and density

hiPSC-RPE cells density and morphology were observed under light microscopy before experiment start (day 0) and at day 1, 5 and 7 after B-27 Supplement starvation (Fig.1a).

Melanin, a black, light absorbing polymer confers pigmentation to RPE cells. In the cell count of pigmented cells at these time-points we did not observe a decrease in pigmented cells between hiPSC-RPE cells cultured in presence or in absence of the B-27 Supplement, only a slight and transient increased number of pigmented cells at day 5 was noted in B-27 Supplement starvation condition ($p=0.0189$) (Fig. 1b). Cell density assessed by DAPI staining showed no differences in both conditions (Fig.2). Also immunocytochemical staining for the junction-specific membrane protein Zonula Occludens 1 (ZO-1) indicating the formation of differentiated polarized RPE cells, remained stable in both cell culture conditions, and the cell exhibited the RPE characteristically polygonal shape with similar cell size (Fig.2).

The expression of mature RPE associated marker (ZO-1, CRALBP) are unaffected in absence of B-27 Supplement. RPE65 expression is reduced. BEST-1 localisation is altered.

Immunofluorescence show similar level of expression of ZO-1, BEST1 and CRALBP in hiPSC-RPE mature RPE associated markers of RPE differentiation after 7 days B-27 starvation in comparison to control conditions.

ZO-1 is a junction-specific membrane protein, its expression suggests the formation of a differentiated polarized RPE culture²⁶ (Fig.2).

RPE65 is an enzyme found in the visual cycle key for the regeneration of 11-cis-retinal, the cone and rod chromophore opsins. Quantification showed lower expression of RPE65 positive cells in B-27 Supplement starvation conditions, hiPSC-RPE cells grown with B-27 showed 40.38% RPE65 positive cells per field, whereas cells without B-27 showed 34.52% RPE65 positive cells per field (n=3) (results not shown).

BEST1, Bestrophin-1, is a membrane protein that functions as a calcium-activated anion channel, reported localized predominantly to the basolateral plasma membrane of the RPE²⁷. BEST1 expression levels greatly varies in RPE cells as exemplified by the in vitro promoter studies of BEST1 expression²⁸. Quantification in B-27 condition showed similar levels of BEST1 positive cells. hiPSC-RPE cells grown with B-27 showed 40.74% BEST1-positive cells per field, whereas hiPSC-RPE cells grown without B-27 showed 39.74% BEST1-positive cells per field (n=3) (results not shown). However, BEST1 localization seemed to be more intracytoplasmic in B-27 Supplement condition.

CRALBP, the cellular retinaldehyde-binding protein, expressed abundantly in the RPE and in the Mueller glial cells of the retina is essential to the visual cycle by carrying 11-cis-retinaldehyde or 11-cis-retinal within the RPE protein complex (Fig. 3)²⁹. Quantification in B-27 condition showed similar expression of CRALBP positive cells in both conditions. hiPSC-RPE cells grown with B-27 showed 56.47% CRALBP positive cells per field whereas in B-27 starvation condition showed 54.84% CRALBP positive cells per field (n=3) (results not shown).

TER values were closer to human RPE measurement in B-27 starvation condition.

To confirm the integrity and permeability of the polarized monolayer TER measurement of electrical resistance across a cellular monolayer were performed. TER appears once RPE monolayers are confluent and polarized with functional tight junctions, it increases before reaching a steady state. In our experiment, monolayer cultures were used when the TER was above $300\Omega\cdot\text{cm}^2$ displaying a mature polarized monolayer. Most RPE TER values come from experiments using monolayer cultures of fetal human RPE (fhrPE) which values reach $>500\Omega\cdot\text{cm}^2$ ^{23,30,31}. However, it is known that TER values can vary between cell lines. In our study, the iPSC-derived RPE cells reached a plateau by $300\Omega\cdot\text{cm}^2$. One day B-27 Supplement starvation, a significant reduction in TER values was noticed, after which the values remained stable along the 7 days observation period ($p=0.02$) (n=2-16) (Fig. 4).

Discussion

RPE cells express ions and water channels as well as insulin receptors³². Insulin is known to act on ions and water channel expression in various organs; ENaC and Kir 4.1/5.1 in the kidney^{14,15}, AQP9 in the placenta¹⁶, but the exact role of insulin in fluid accumulation in the retina leading to DME formation has not been fully studied to date. We conducted this systematic analysis on human induced pluripotent stem cell (hiPSC) derived into RPE to obtain a RPE cell model in insulin-free culture conditions opening the path to future studies of the effects of insulin on the retinal barriers and their drainage mechanisms.

We noticed that the widely used B-27 Supplement for RPE cell culture contains high levels of insulin. According to published formulas for neuronal cell culture we estimated the concentration of insulin to be between 3-5 $\mu\text{g}/\text{ml}$ ^{24,25}. These insulin concentrations are extremely high as fasting insulin level in healthy human is close to 1 ng/ml ³³. This finding underlies the importance of controlling the concentration of any compound used for experimentation. While it is certainly convenient to rely on commercially available supplement such as B-27 Supplement, however having no control on the dosage of each various components can be a disadvantage. In our study, the confidentiality of the composition prevented us to produce and test an insulin-free B-27 Supplement. Therefore, cells starved from the other components included in the B-27 Supplement eventually affecting the outcome. However, we did not observed common reported problems with serum-free medium such as cells detachment from the support, probably due to the MRF-coating³⁴.

Within the 7 days of experiment, we observed no morphological, cell density or CRABLP, BEST1 protein expression variation in absence of B-27 Supplement. During starvation, tight junctions were maintained creating a concentration gradient between apical and basal environments. Interestingly the observed TER values in B-27 Supplement starvation conditions were lower and closer to reported fresh native human RPE TER values 150 $\Omega\cdot\text{cm}^2$ ³⁵. The TER value remained stable and did not continue to drop further indicated a potential role of the ion composition of the media in the TER measurement.

Only a discrete and transient superiority in number of pigmented cells was noted in the B-27 starvation group. Transferrin and thereby iron contained in B-27 Supplement is an essential metal ion for the RPE65 isomerohydrolase activity³⁶. Thus, we could suppose that the 14% decrease we observed in RPE65 expression is due to the absence of this ferrous ion.

In conclusion, our findings reveal that B-27 Supplement-free culture media is possible to test insulin effects in hiPSC-RPE cell model. Further studies will need to investigate how B-27 starvation influence protein level and RNA expression levels.

Bibliography

1. International Diabetes Federation. IDF Diabetes Atlas, 8th edn. Brussels, Belgium: International Diabetes Federation, 2017
2. Congdon NG, Friedman DS, Lietman T. Important causes of visual impairment in the world today. *JAMA* 290: 2057–60, 2003
3. Gonder JR, Walker VM, Barbeau M, et al. Costs and quality of life in diabetic macular edema: Canadian Burden of Diabetic Macular Edema Observational Study (C-REALITY). *J Ophthalmol* 1–9, 2014
4. Varma R, Bressler NM, Doan QV, et al. Prevalence of and risk factors for diabetic macular edema in the United States. *JAMA Ophthalmol.* 132(11):1334-40, 2014
5. Klein R, Klein B, Scot E, et al. The Wisconsin Epidemiologic Study of Diabetic Retinopathy: IV. Diabetic Macular Edema. *JAMA Ophthalmol.* 91(12), 1464-1474, 1984
6. Bhagat N, Grigorian RA, Tutela A et al, Diabetic Macular Edema: Pathogenesis and Treatment. *Survey of Ophthalmology*, 54(1), 2009
7. American Diabetes Association. Standards of medical care in diabetes—2016. *Diabetes Care* S1-S106;39(suppl 1), 2016
8. Zhao C, Wang W, Xu D et al. Insulin and risk of diabetic retinopathy in patients with type 2 diabetes mellitus: data from a meta-analysis of seven cohort studies. *Diagn Pathol.*9:130, 2014
9. Henricsson M, Janzon L, Groop L. Progression of retinopathy after change of treatment from oral antihyperglycemic agents to insulin in patients with NIDDM. *Diabetes Care.*18(12):1571-6, 1995
10. The Effect of Intensive Treatment of Diabetes on the Development and Progression of Long-Term Complications in Insulin-Dependent Diabetes Mellitus. *NEngl J Med* 329: 977–86, 1993
11. Klaassen I, Van Noorden CJ, Schlingemann RO. Molecular basis of the inner blood-retinal barrier and its breakdown in diabetic macular edema and other pathological conditions. *Prog Retin Eye Res.* 34:19-48, 2013
12. Tran TL, Bek T, Holm L et al. Aquaporins 6-12 in the human eye. *Acta Ophthalmol.* 91(6):557-63, 2013
13. Krueger B, Schlotzer-Schrehardt U, Haerteis S et al. Four subunits ($\alpha, \beta, \gamma, \delta$) of the epithelial sodium channel (ENaC) are expressed in the human eye in various locations. *Invest Ophthalmol Vis Sci.* 53(2):596-604, 2012
14. Li L, Garikepati RM, Tsukerman S, Kohan D, Wade JB, Tiwari S, et al. Reduced ENaC activity and blood pressure in mice with genetic knockout of the insulin receptor in the renal collecting duct. *Am J Physiol Renal Physiol.* 304(3):F279-88, 2013
15. Zaika O, Palygin O, Tomilin V et al. Insulin and IGF-1 activate Kir4.1/5.1 channels in cortical collecting duct principal cells to control basolateral membrane voltage. *Am J Physiol Renal Physiol.* al 00436, 2015
16. Castro Parodi M, Farina M, Dietrich V et al. Evidence for insulin-mediated control of AQP9 expression in human placenta. *Placenta.* 32(12):1050-6, 2011
17. Takahashi, K., Yamanaka, S. Induction of pluripotent stem cells from mouse embryonic and adult fibroblast cultures by defined factors. *Cell*, 126(4), 663–676. 2006
18. Takahashi, K., Tanabe, K., Ohnuki, M. et al.. Induction of pluripotent stem cells from adult human fibroblasts by defined factors. *Cell*, 131(5), 861–872. 2007
19. Brewer GJ, Torricelli JR, Evege EK et al. Optimized Survival of Hippocampal Neurons in B27-Supplemented Neurobasal, a New Serum-free Medium Combination. *Journal of Neuroscience Research* 35:567-576, 1993
20. Romijn HJ. Towards an improved serum-free, chemically defined medium for long-term culturing of cerebral cortex tissue. *Neurosci Biobehav Rev.* Fall;8(3):301-34, 1984.
21. Romijn HJ. Development and advantages of serum-free, chemically defined nutrient media for culturing of nerve tissue. *Biol Cell.* 63(3):263-8, 1988
22. Okita K, Matsumura Y, Sato Y, et al. A more efficient method to generate integration-free human iPS cells. *Nat Methods.* 8: 409–412, 2011
23. Sanoda S, Spee C, Barron E et al. A protocol for the culture and differentiation of highly polarized human retinal pigment epithelial cells. *Nature Protocole* 4(5): 662–673.12, 2009
24. Hanna Lab Protocol Weizmann Institute of Science Ver. 2 - Last updated: 17/02/2016
25. Bottenstein J, Sato G. Growth of a rat neuroblastoma cell line in serum-free supplemented medium. *Proc. Natl. Acad. Sci. USA* Vol. 76, No. 1, pp. 514-517, *Neurobiology* January 1979
26. Sanoda A JM, Van Itallie CM. Tight junctions and the molecular basis for regulation of paracellular permeability. *Am J Physiol* 269:G467–475. 1995
27. Reichhart N, Strauss O. Ion channels and transporters of the retinal pigment epithelium. *Experimental Eye Research* 126 27e37, 2014
28. Iacovelli J, Zhao C, Wolkow N et al. Generation of Cre Transgenic Mice with Postnatal RPE-Specific Ocular Expression. *Investigative Ophthalmology & Visual Science*, Vol. 52, No. 3 1378, 2011
29. Strauss O. The Retinal Pigment Epithelium in Visual Function. *Physiol Rev* 85: 845–881, 2005
30. Brandl C, Zimmermann SJ, Milenkovic VM et al. In-depth characterisation of Retinal Pigment Epithelium (RPE) cells derived from human induced pluripotent stem cells (hiPSC). *Neuromolecular Med.* Sep;16(3):551-64, 2014
31. Sheller RA, Cuevas ME, Todd MC. Comparison of transepithelial resistance measurement techniques: Chopsticks vs. Endohm. *Biol Proced Online.* 19:4. 2017
32. Sugasawa K, Deguchi J, Okami T et al. Immunocytochemical analyses of distributions of Na,K-ATPase and GLUT1, insulin and transferrin receptors in the developing retinal pigment epithelial cells. *Cell Struct Funct* 19: 21–28, 1994
33. Melmed S, Polonskiy KS, Larsen PR et al. Textbook of Endocrinology. 12th ed. Philadelphia: Elsevier Saunders; 2011
34. ATCC® Animal cell culture guide, 2014
35. Quinn RH, Miller SS. Ion Transport Mechanisms in Native Human Retinal Pigment Epithelium. *Investigative Ophthalmology & Visual Science*, Vol. 33, No. 13, December 1992
36. Moiseyev G, Takahashi Y, Chen Y et al. RPE65 is an iron(II)-dependent isomerohydrolase in the retinoid visual cycle. *J Biol Chem.* 281(5):2835-40, 2006

Figure 1a. Pigmented cell count hiPSCs-RPE from day 0 to day 7. Light microscope images show discret more pigmented cells at day 5 in B-27 starvation condition, but no change in morphology or cell density. Magnification 20X.

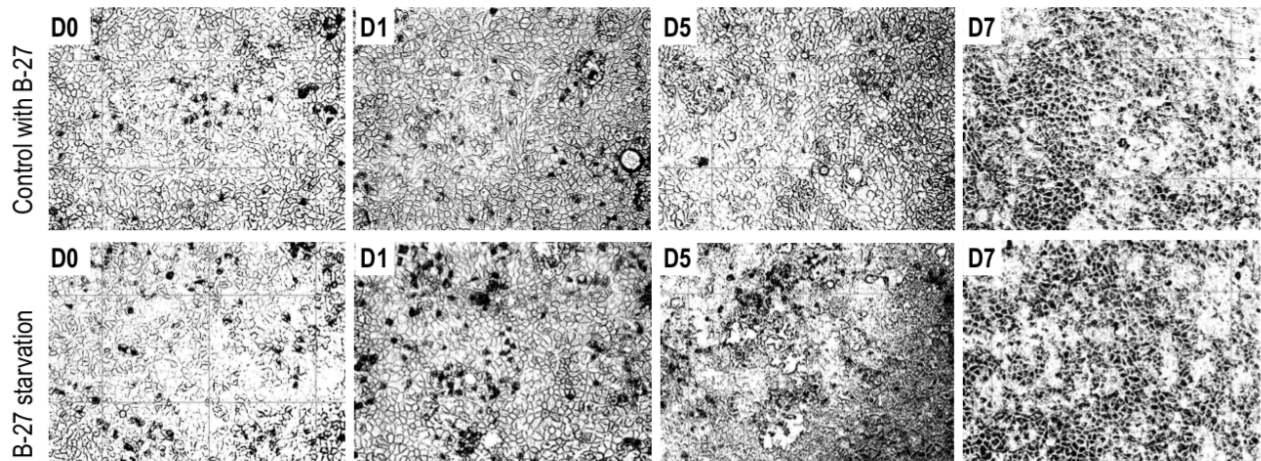


Figure 1b. Pigmented cell count hiPSCs-RPE from experimental day 0 to day 7. Light microscope images show significantly more pigmented cells at day 5 in B-27 starvation condition ($p=0.0189$), but no change in morphology or cell density ($n=6$). The arrow represents the medium change. Results are expressed in percentage of pigmented cells per field.

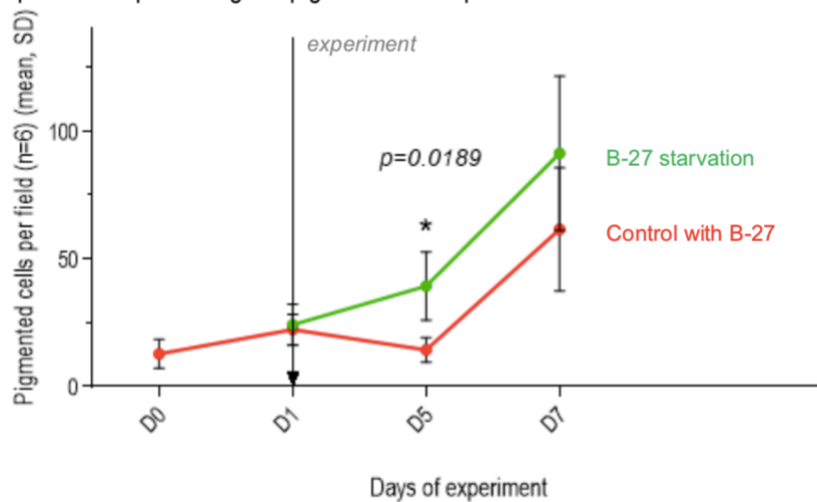


Figure 2. Nucleus density and cell morphology of hiPSCs-RPE cells after 7 days B-27 starvation. Nucleus DAPI staining binding to cellular DNA (left panels) reveal similar nucleus density as in control condition, ZO-1 (zona-occludens-1) a scaffold protein forming tight junction in RPE cells staining (right panels) reveal comparable cell morphology after 7 days B-27 starvation as in control conditions. Expression of ZO-1 suggests formation of a polarized RPE monolayer (Strauss, 2014). Fluorescence microscope images at 20X magnification, pictures taken with DAPI at 10ms exposure, with ZO-1 at 500ms exposure.

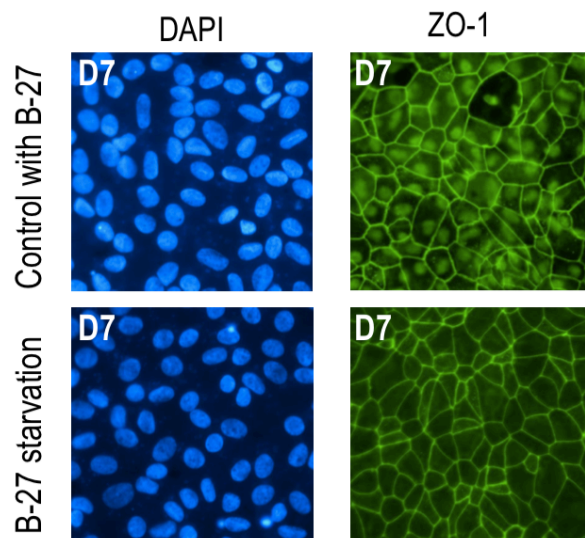


Figure 3. Immunofluorescence show same intensity of hiPSCs-RPE typical metabolic markers after 7 days B-27 starvation in comparison to control conditions. **RPE65** a key enzyme found in the visual cycle for regeneration of 11-cis-retinal is used as visual chromophore both by cone and rod photoreceptors. Its expression is reduced in the B-27 starvation group. **BEST-1**, Bestrophine-1, is a membrane calcium-activated anion channel which expression in the RPE cells is described mainly on the basolateral membrane. In B-27 Supplement condition it seems to have an intracytoplasmic distribution. **CRALBP**, cellular retinaldehyde-binding protein, a visual cycle protein is found in the RPE cytosol. Magnification 40X.

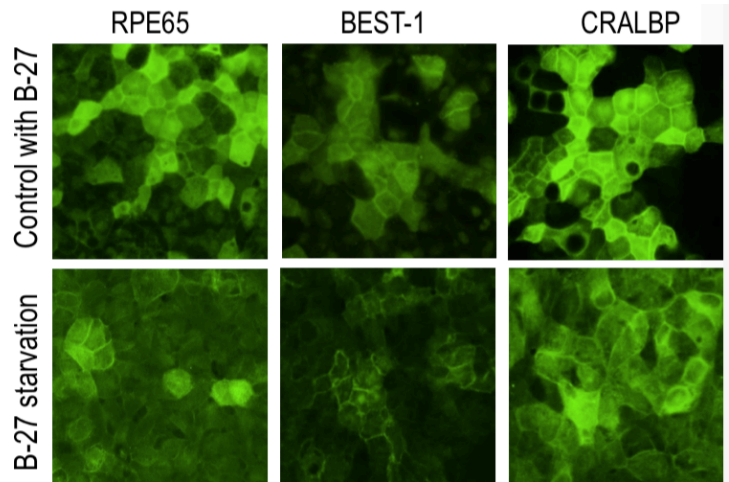
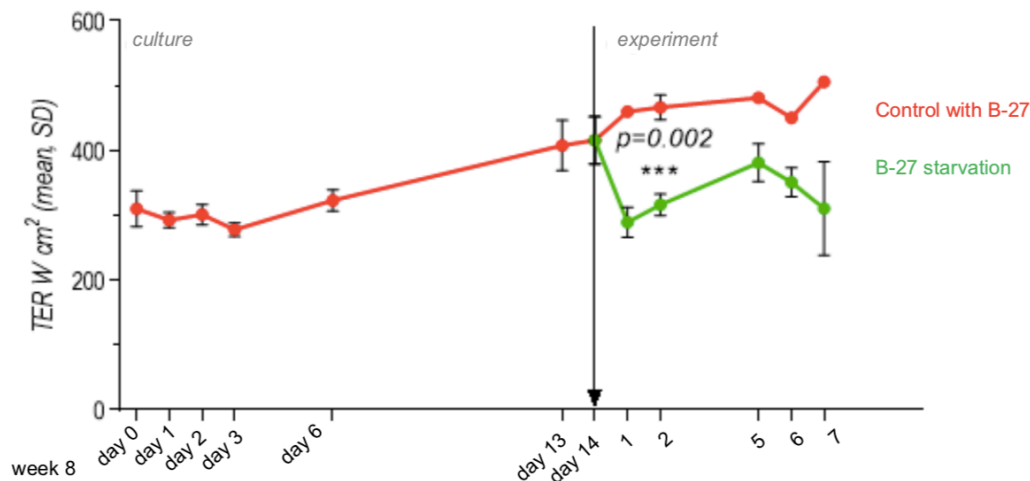


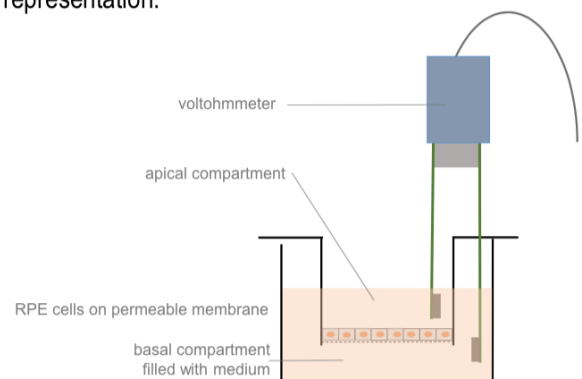
Figure 4. Transepithelial resistance (TER) values of electrical resistance across the hiPSCs-RPE cellular monolayer showing a polarization between basolateral and apical compartments. During the 8th cell culture week we observed a stable, slowly rising TER. Follow-up during the 7 days experiment. At experimental day 1 B-27 starved conditions exhibit significant inferior TER values with $289.40 \pm 10.49 \Omega \cdot \text{cm}^2$ (green, lower line) in comparison with control conditions $460 \pm 1.00 \Omega \cdot \text{cm}^2$ (red, upper line) ($p=0.002$).



Tab 1. Values represent transepithelial resistance measurements in mean \pm standard error of the mean during cell culture and during the 7 days experiment in B-27 starvation conditions. Values are shown in $\Omega[\text{Ohms}] \cdot \text{cm}^2$. The remaining 9 wells (out of 16) were used for immunocytochemistry assay.

Transepithelial resistance in culture with B-27 [$\Omega \cdot \text{cm}^2$]			
days in culture at	Mean	SEM	n
week 8	310.00	6.88	16
day 1	292.63	2.95	16
day 2	301.19	3.86	16
day 3	277.81	2.61	16
day 6	322.94	4.16	16
day 13	407.69	9.74	16
day 14	416.00	9.10	16
Control condition with B-27			
days of experiment	Mean	SEM	n
1	460.00	1.00	2
2	466.50	13.50	2
5	481.50	1.50	2
6	450.50	2.50	2
7	506.00	2.00	2
B-27 Starvation			
days of experiment	Mean	SEM	n
1	289.40	10.49	5
2	316.20	7.48	5
5	381.20	12.95	5
6	351.00	9.88	5
7	310.80	32.37	5

Suppl. Figure 1. Transepithelial electric resistance measurement and transwell culture system in schematic representation.





UNIL | Université de Lausanne

Faculté de biologie
et de médecine

Annexes

Thèse de doctorat en médecine de Lilly Khamsy
préparée sous la direction de Professeure Francine Behar-Cohen

Annexe 3 : présentation au congrès ARVO 2017

CONTROL ID: 2691980

SUBMISSION ROLE: Abstract Submission

AUTHORS

AUTHORS (LAST NAME, FIRST NAME): khamisy, lilly^{1, 2}; Kowalczyk, Laura^{1, 2}; Favez, Tatiana¹; Martin, Catherine¹; Behar-Cohen, Francine F.^{1, 2}

INSTITUTIONS (ALL):

1. HOJG, Lausanne, Switzerland.
2. Ophthalmology, University of Lausanne, Lausanne, Switzerland.

Commercial Relationships Disclosure (Abstract): lilly khamisy: Commercial Relationship: Code N (No Commercial Relationship) | Laura Kowalczyk: Commercial Relationship: Code N (No Commercial Relationship) | Tatiana Favez: Commercial Relationship: Code N (No Commercial Relationship) | Catherine Martin: Commercial Relationship: Code N (No Commercial Relationship) | Francine Behar-Cohen: Commercial Relationship: Code N (No Commercial Relationship)

Study Group: (none)

ABSTRACT

TITLE: The role of insulin in diabetic retinal homeostasis.

ABSTRACT BODY:

Purpose: Type 2 diabetic insulin-resistant patients have high insulin circulating levels and insulin treatment is potentially aggravating the risk of retinopathy and macular edema. But the exact direct role of insulin on hydro-ionic retinal homeostasis remains incompletely understood. The aim of this study is to analyze the effect of insulin on human retinal pigment epithelium (RPE) cells in hyperglycemic conditions in vitro and after intravitreal injection in Goto Kakizaki (GK) type 2 diabetic rats.

Methods: ARPE19 cell line and human induced pluripotent stem cells derived into RPE (iPSc-RPE) were used to evaluate tight junction (TJ) rearrangement in hyperglycemic conditions in presence of insulin in vitro. Cell viability and proliferation were analyzed. Immunofluorescence of Zona occludens-1 staining was performed after 7 days of treatment in high glucose (40mM) and high insulin (10nM, 100nM) conditions following 24h FBS starvation. In parallel, transepithelial resistance (TER) measurements was performed. In vivo, insulin was injected in the vitreous of GK rats and 150kDa FITC dextran was injected intravenously one hour prior to sacrifice (n=6). Glycemia levels were recorded.

Results: ARPE19 and iPSc-RPE cell monolayer form TJ thus maintaining a concentration gradient between apical and basal environments. We validated the presence of functional insulin receptors in our cell cultures. Insulin (10nM) induces cell proliferation. We consistently see opening of TJ in high glucose (40mM) and high insulin (10nM) conditions after 7 days of treatment compared with baseline conditions in which ARPE19 cells exhibit intact cobblestone appearance (glucose 25mM, insulin 0nM). Paradoxically TER increased in high glucose and high insulin conditions in which opening of TJ was seen. B27 supplement starvation in iPSc-RPE cultures reduced TER. Interestingly, higher insulin (100nM) levels did not induce opening of TJ, suggesting involvement of a pathway dependent on insulin receptor regulation. In vivo, insulin injected intravitreally in GK diabetic rats induced retinal vessels vasodilation and leakage. No glycemic changes resulted from intravitreal injection of insulin.

Conclusions: Our findings reveal that insulin in combination with high glucose impairs TJ arrangement in RPE. In vivo, high levels of insulin in the vitreous may be responsible for aggravation of macular edema.

(No Image Selected)

DETAILS

PRESENTATION TYPE: Poster Only

CURRENT REVIEWING CODE: 1940 diabetic retinopathy: cell biology - RC

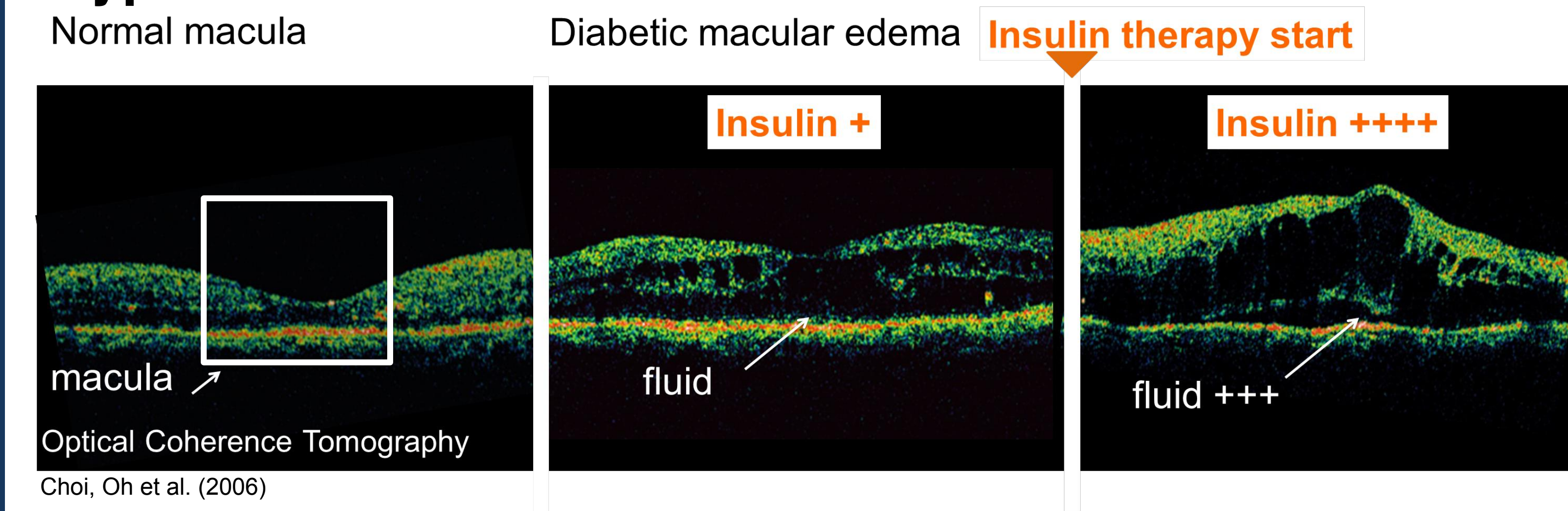
CURRENT SECTION: Retinal Cell Biology

The role of insulin in diabetic retinal homeostasis

Introduction

Type 2 diabetic insulin-resistant patients have high insulin circulating levels, and insulin treatment initiation transiently **aggravates** the risk of retinopathy and macular edema. But the exact direct role of insulin on hydro-ionic retinal homeostasis remains incompletely understood.

Hypothesis



Goals

- Understand **insulin's** influence in hyperglycemic conditions on :
- blood retinal barrier breakdown
 - ion and channel localisation and expression in human RPE cells

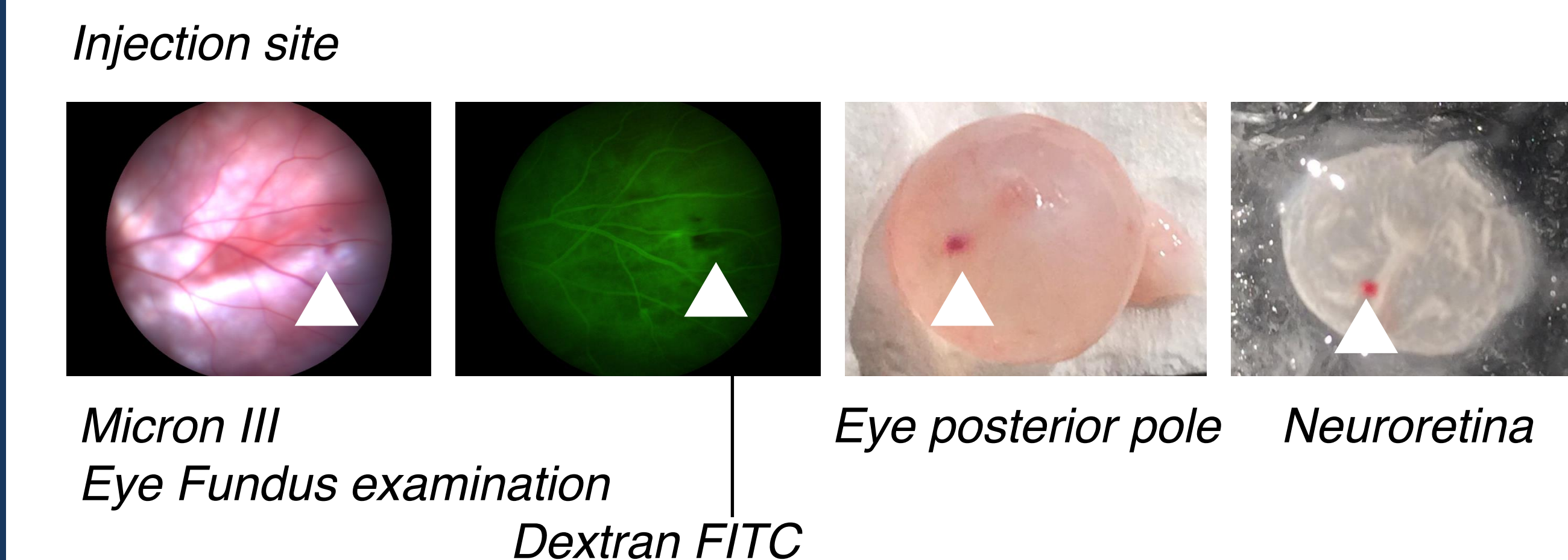
Methods

In vitro : ARPE19, iPSc-RPE

ARPE19 cell line and human induced pluripotent stem cells derived into RPE (iPSc-RPE) were used to **evaluate tight junction (TJ) rearrangement** in hyperglycemic (6,6mM, 21.23mM or 40mM) conditions in presence of insulin (10nM, 100nM) (n=3). Before treatment ARPE19 cells were FBS starved 24h, iPSc-RPE cells were starved from B27 supplement during 14 days. Mannose was used for osmotic control of equal molecular weight. Cell viability and proliferation were analyzed. Immunofluorescence of Zona occludens-1 staining was performed. qPCR for occludin mRNA was performed, RPL8 was used as reference.

In vivo : Goto Kakizaki – type 2 diabetes rat

Insulin 100nM was injected intravitreally (IVT) in both eyes of 6 months old diabetic rats (n=6). 150 kDa FITC dextran was injected intravenously one hour prior to sacrifice (n=6). Glycemia levels were recorded. Fundus examination and OCT was performed after IVT. Post mortem cryosection were performed.

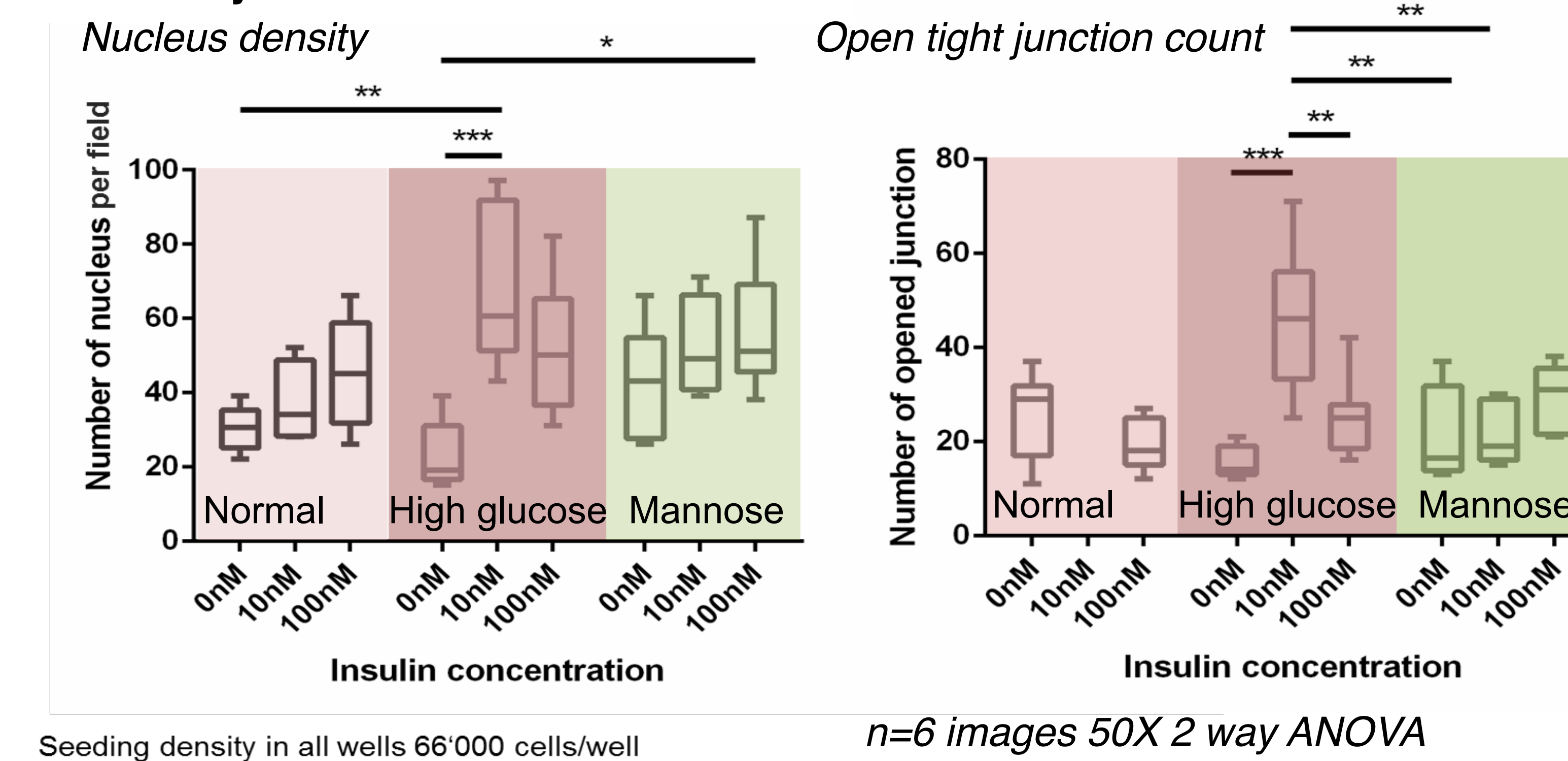


Results in vitro

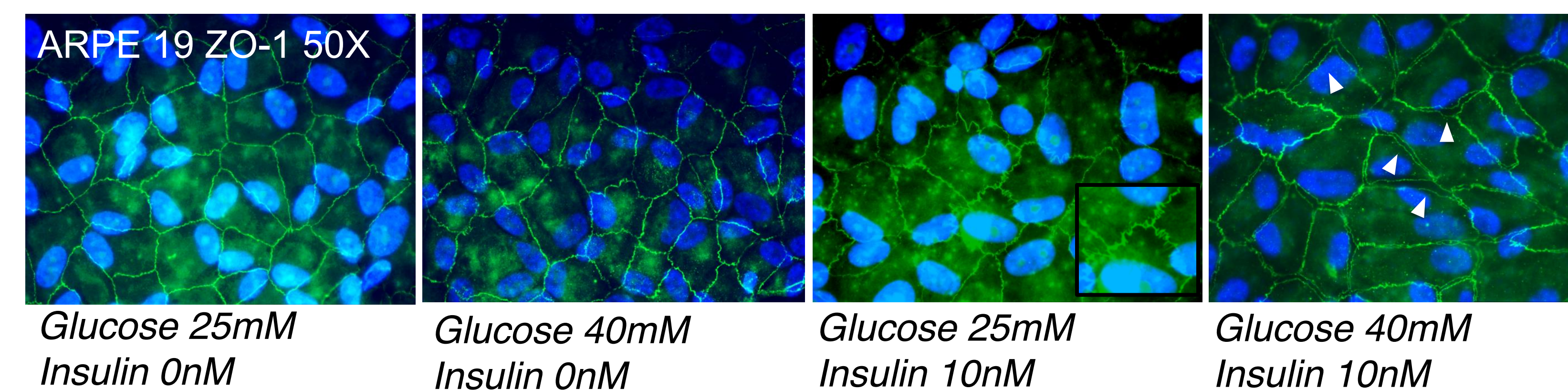
ARPE19 and iPSc-RPE cell grew in monolayer forming **TJ** creating a concentration gradient between apical and basal environments.

ARPE19

Opening of TJ in high glucose (40mM) and high insulin (10nM) conditions after 7 days of treatment.

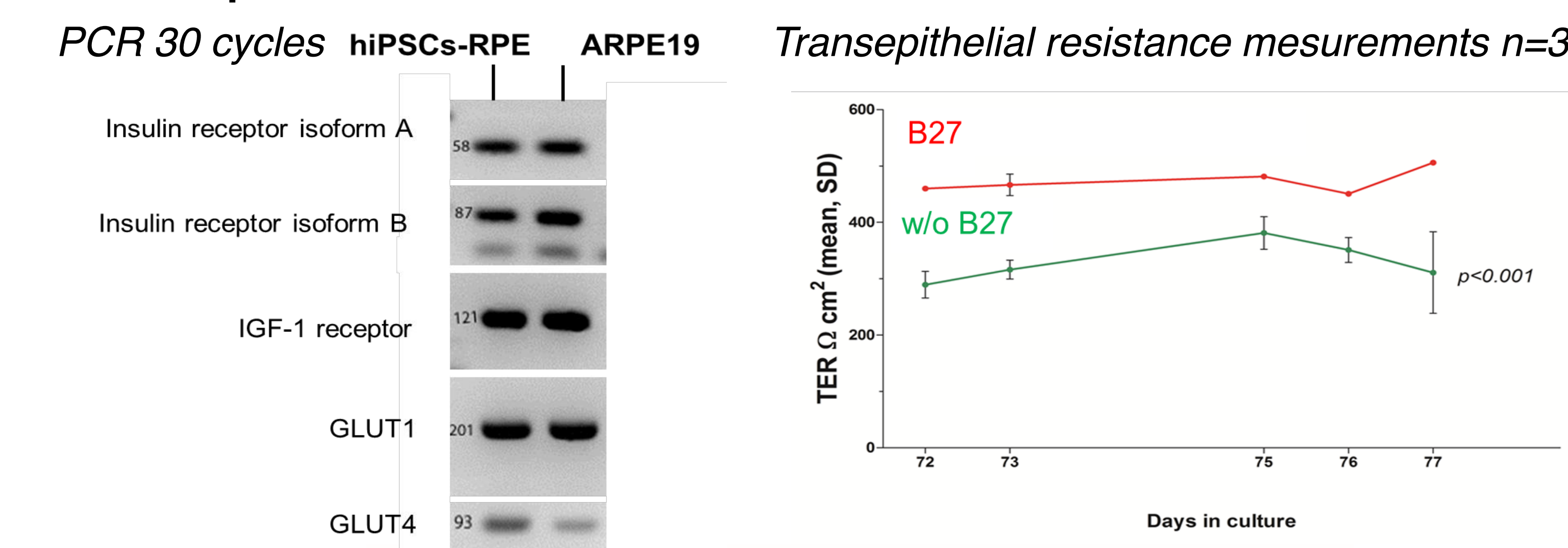


→ **Higher insulin (100nM) levels did not induce opening of TJ, suggesting the involvement of a pathway dependent on insulin receptor regulation.**

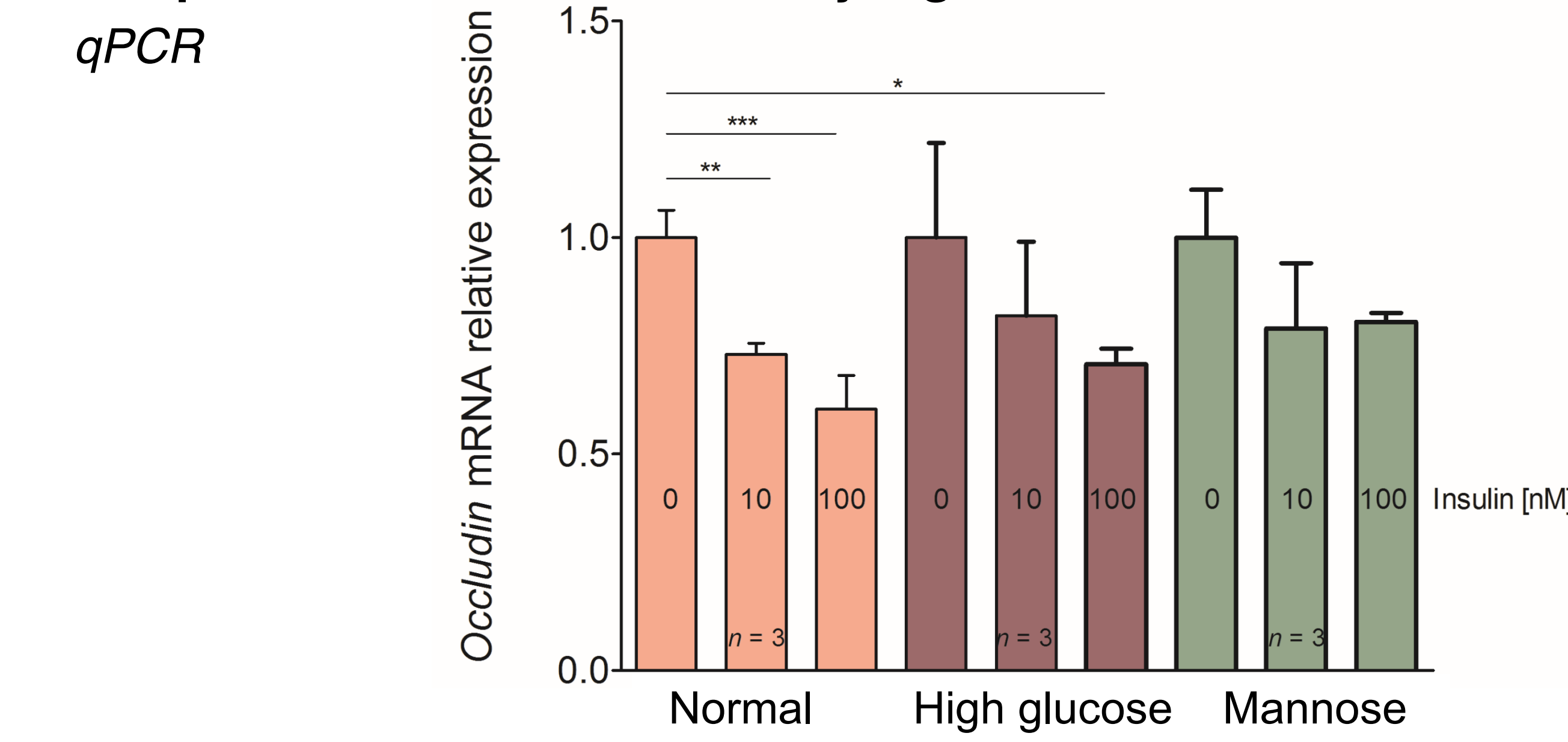


iPSc-RPE

→ **Presence of functional insulin receptors**
→ **B27 supplement (containing >500nM insulin) starvation reduces Transepithelial resistance**

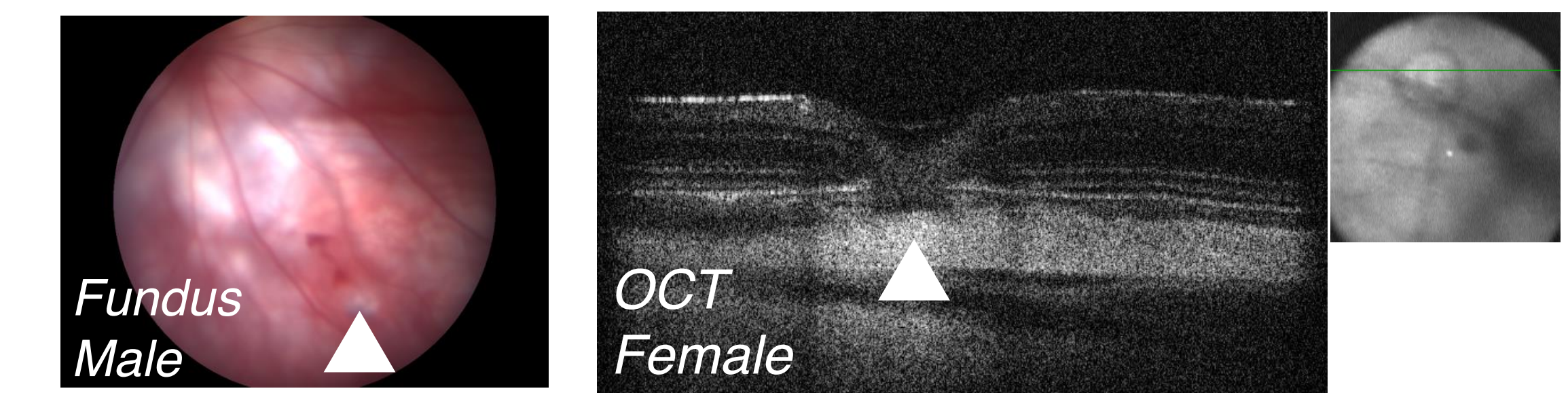


→ **TJ protein occludin reduced by high insulin after 24h treatment**

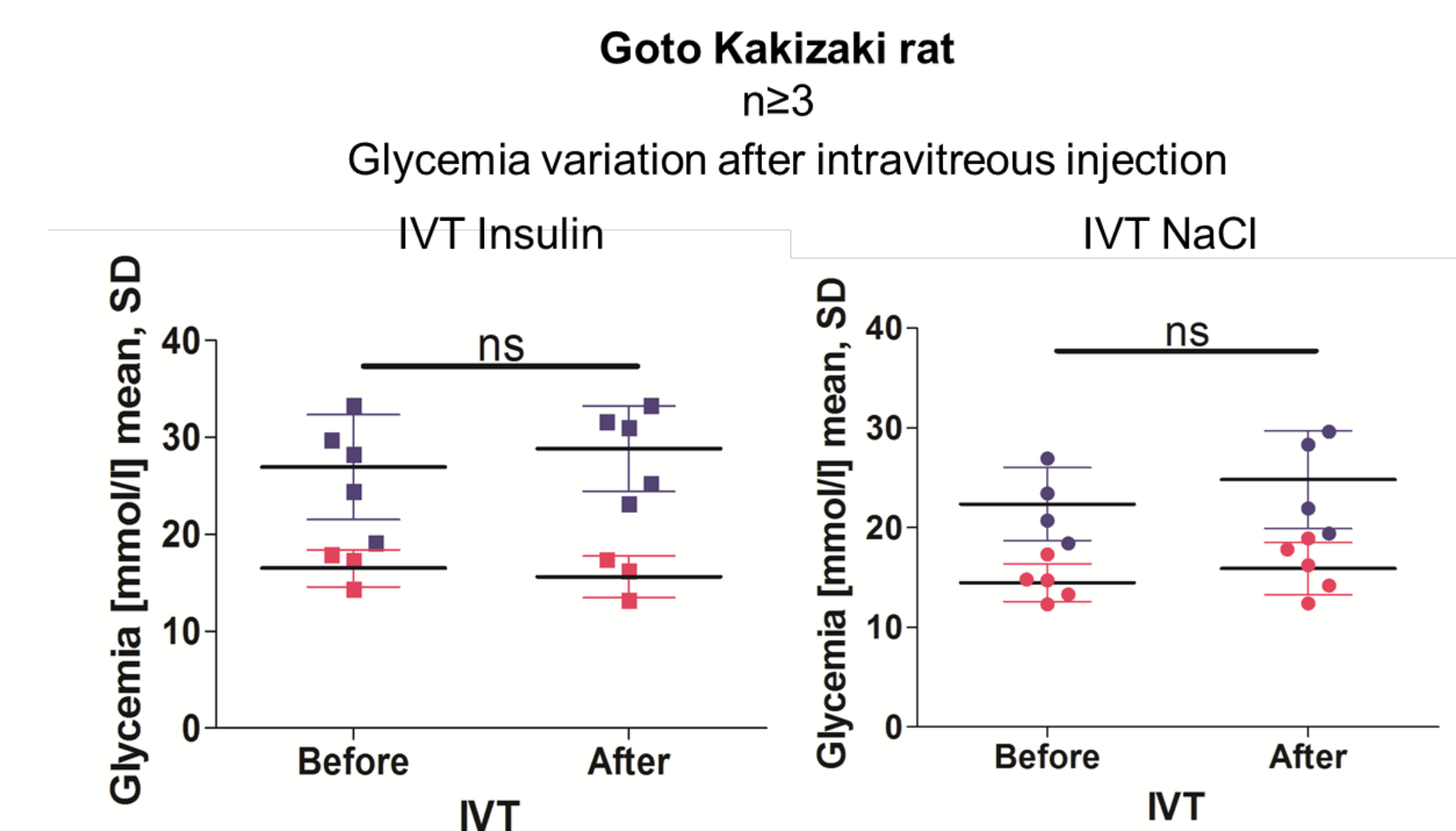


Results in vivo

Exclusion 2 eyes due to hemorrhage or retinal detachment.



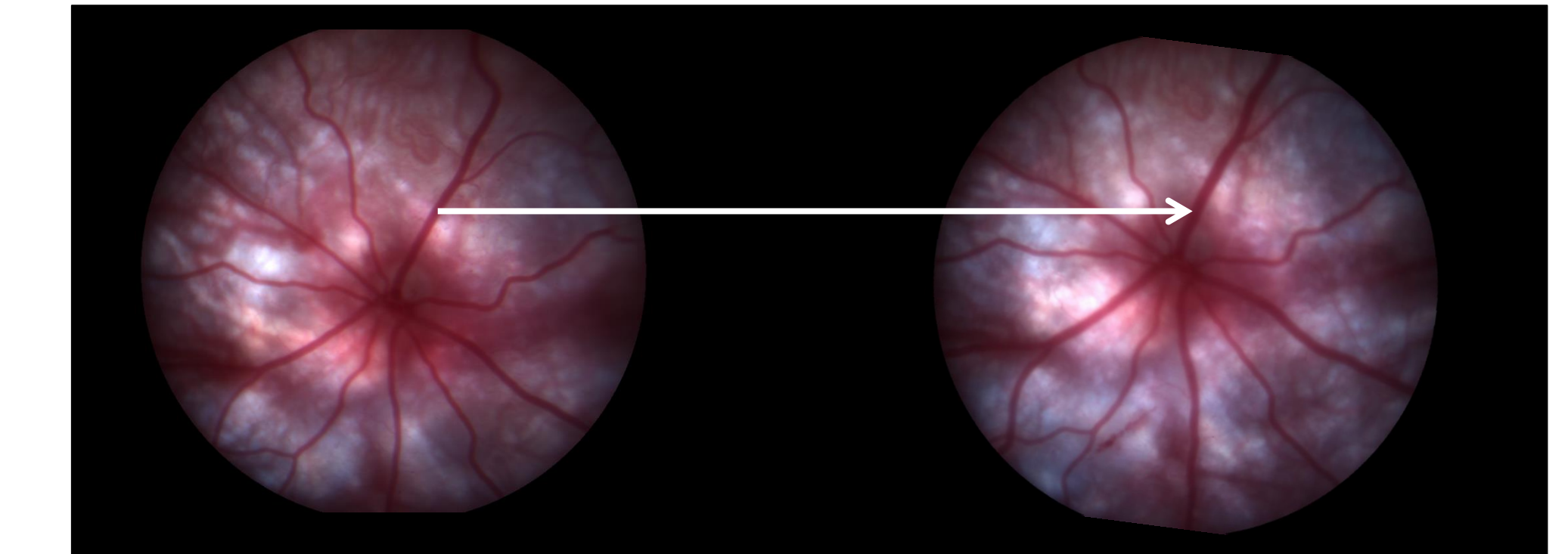
No glycemic changes resulted from intravitreal injection of insulin.



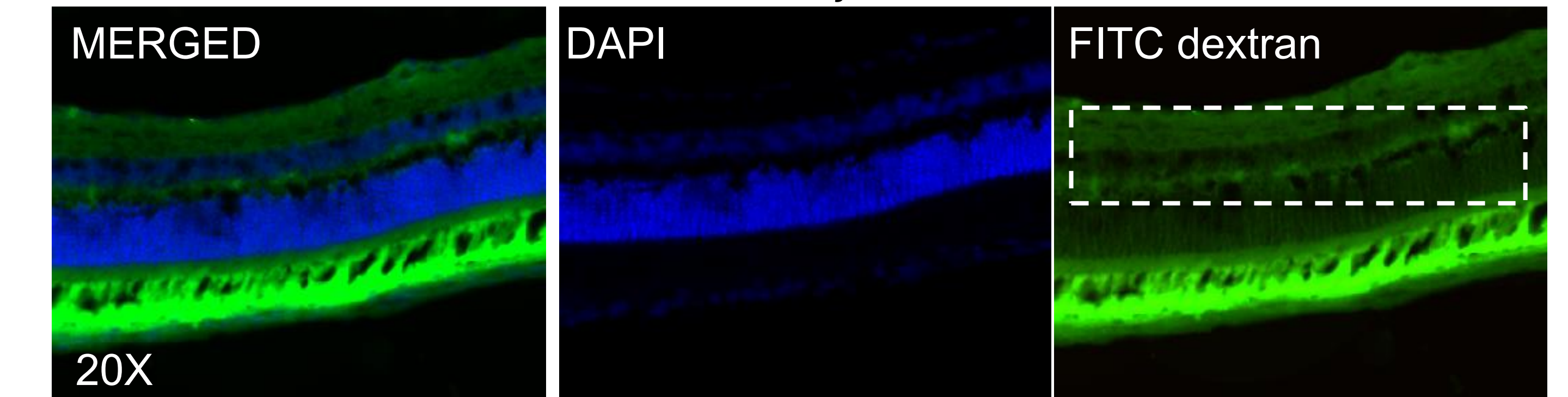
Systemic Glycemic variation after IVT injection Insulin 100nM vs NaCl 0.9%

→ **In vivo, insulin injected intravitreally in GK diabetic rats induced retinal vessels vasodilation and leakage.**

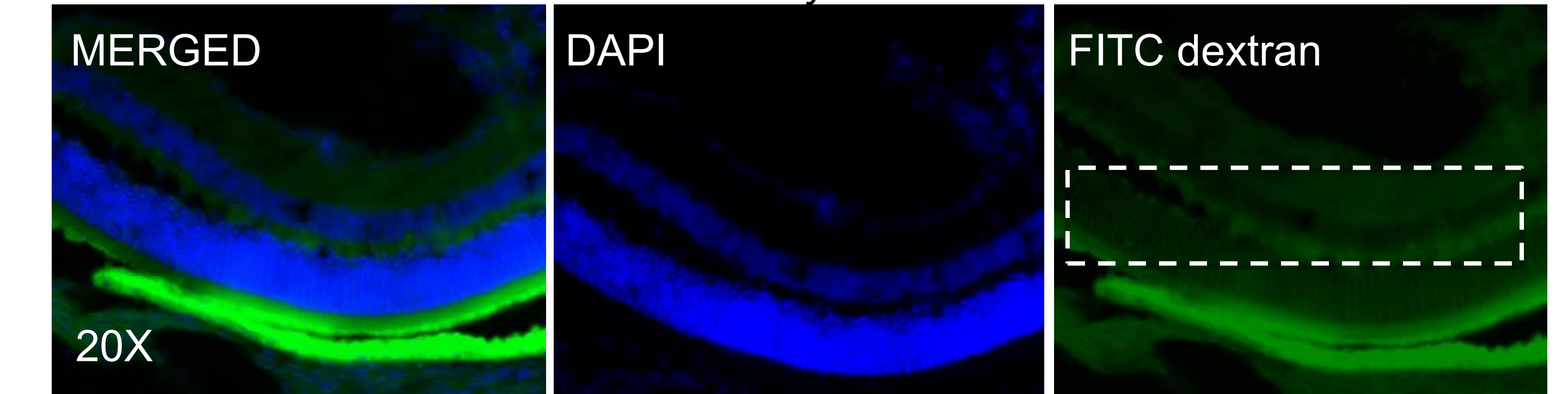
Insulin IVT in female diabetic rat 6 months old fundus



Insulin IVT in male diabetic rat 6 months old cryosection



NaCl IVT in male diabetic rat 6 months old cryosection



Conclusion

- Insulin in combination with high glucose impairs TJ arrangement in RPE
- In vivo, high levels of insulin in the vitreous may be responsible for aggravation of macular edema





UNIL | Université de Lausanne

Faculté de biologie
et de médecine

Annexes

Thèse de doctorat en médecine de Lilly Khamsy
préparée sous la direction de Professeure Francine Behar-Cohen

Annexe 4 : publication Molecular Vision

Glial cells of the human fovea

Kimberley Delaunay,¹ Lilly Khamsy,² Laura Kowalczyk,² Emmanuelle Gelize,¹ Alexandre Moulin,² Michaël Nicolas,² Leonidas Zografos,² Patricia Lassiaz,¹ Francine Behar-Cohen^{1,3,4}

(The first two authors have contributed equally to this study.)

¹Centre de Recherche des Cordeliers INSERM, Physiopathology of ocular diseases team, Université de Paris, Université Sorbonne Paris Cité, Paris, France; ²Department of Ophthalmology, University of Lausanne, Jules-Gonin Eye Hospital, Fondation Asile des aveugles, Lausanne, Switzerland; ³Hopital Cochin, Ophthalmopole, Assistance Publique - Hôpitaux de Paris, France; ⁴Université de Paris, France

Purpose: The exact cellular types that form the human fovea remain a subject of debate, and few studies have been conducted on human macula to solve this question. The purpose of this study was to perform immunohistochemistry on fresh human samples to characterize the glial cells that form the human fovea.

Methods: Immunohistochemistry was performed using antibodies against proteins expressed in astrocytes or in retinal Müller glial cells or both types of cells on six human macula obtained from eyes enucleated for peripheral intraocular tumors and on two postmortem eyes from healthy donors. The posterior poles of the enucleated eyes were cryosectioned and stained with antibodies against the glial proteins GFAP, vimentin, CRALBP, glutamine synthetase, and connexin 43.

Results: A population of cells positive for GFAP and negative for glutamine synthetase and CRALBP that express connexin 43 were identified at the roof of the foveal pit. These cells are distinct from the Müller cone cells described by Yamada and Gass, suggesting that another type of foveal glial cells, most likely astrocytes, are present in the human fovea.

Conclusions: This study showed that in humans, astrocytic glial cells cover the foveal pit. Their roles in macula homeostasis and mechanisms of macular disease remain to be determined.

The human macula is a highly specialized retinal area, located at the center of the visual axis that comprises less than 5% of the total retinal surface. The macula ensures visual acuity and photopic and color vision. With the development of imaging technologies, such as spectral domain optical tomography technology (SD-OCT), the macula morphology is being extensively explored and described in healthy and pathological conditions. In contrast, literature on the histology of the human macula is scarce due to the limited access to fresh human eyes. To improve the interpretation of OCT imaging, a better understanding of the cells that form the macula and the fovea is needed.

The macula is an area 5.5–6.0 mm in diameter, where the ganglion cell layer (GCL) is the thickest of the whole retina [1]. It is divided in concentric regions defined by the number of nuclei in the different cellular layers and by the orientation of the fibers in the outer plexiform layer. In the fovea, which is 1.5 mm in diameter, there are only cones (around 0.3% of the total number of cones). Their density is highest at the foveola where it reaches around 200,000/mm² with high interindividual variability [2]. In the foveola, there are only

cones and retinal Müller glial (RMG) cells and one or two rows of inner nuclei but no nerve fiber layer, no GCL and no inner plexiform layer, as these layers are displaced laterally. In the monkey fovea, equal numbers of Müller cell trunks and cone terminals were described with each Müller cell partially coating two to three cone terminals [3]. Thus, the density of RMG cells is higher in the fovea, where there are only cones. The parafovea is the region (500 µm in diameter around the fovea) with the largest fiber layer and a thick Henle's layer where RMG cells have a Z shape and are bound with cone axons by junction proteins [4].

During development of the retina, the macula forms progressively and continues maturing during childhood until the age of 10–12 years [5]. Astrocytes appear first near the optic disc, and by migrating subsequently further peripherally, they guide the vessels' development, avoiding the fovea that remains avascular during retinal angiogenesis [6,7]. The glial composition of the macula is thought to be exclusively composed of RMG cells. However, the structure of the macroglial cells in the fovea differs from that of the RMG cell structure in other parts of the retina. In 1969, E. Yamada reported the electron microscopy observation of a human retina where he described that the inner half of the foveola was composed of an inverted cone-shaped zone of RMG cells, which was called the "Müller cells cone" (MCC) Interestingly, in this description, a few nuclei of some "atypical glial

Correspondence to: Francine Behar-Cohen, Centre de Recherche des Cordeliers, Inserm U 1138, Physiopathology of ocular diseases: Therapeutic innovations, 15 rue de l'École de Médecine 75006 Paris, France

cells” were observed within the MCC, while the exact location of the foveal MCC cell nuclei was not identified. Yamada also reported that the inner limiting membrane (ILM) at the inner surface of the MCC was much thinner (10 nm to 20 nm) compared to the ILM in the perifoveal region [8], although the density of the RMG cells in this region is high. In 1999, D. Gass supported the existence of the MCC and hypothesized that it could serve as a reservoir for macular pigments, a plug for the maintenance of foveal cones, and that it could explain the pathogenesis of congenital foveoschisis and of age-related macular hole [9]. More recently, Govetto et al. showed that RMG cells in the MCC were stained differently by toluidine blue than other RMG cells on semithin sections of two human maculas and one monkey macula. They explained the foveal cone traction occurring in epiretinal membrane retraction, by the vertical traction of the cone RMG cells [10]. In this observation, the exact location of the vertical RMG cells nuclei was also not clearly identified. Finally, in the monkey retina, a recent immunohistochemistry study raised the possibility that another type of glial cells, probably astrocytes, might exist in addition to RMG cells in the MCC of non-human primates [11].

However, the structure and cellular glial composition of the human fovea remains a subject of debate. To provide additional information on glial cells of the human macula, we performed immunohistochemical analysis of human maculas using RMG and astrocyte markers.

METHODS

Human ocular tissues: The use of human samples adhered to the tenets of the Declaration of Helsinki and was approved by the local Ethics Committee of the Swiss Department of Health on research involving human subjects (CER-VD N°340/15) that the study adhered to the ARVO statement on human subjects. The subjects signed informed consent. Postmortem whole globes were received from the Lausanne Eye Bank, when the cornea had been considered unsuitable for transplantation. Table 1 summarizes information on the ocular samples. Five retinas were obtained from eyes enucleated between 2013 and 2018 for anterior uveal tumors or for conjunctival epidermoid carcinoma but an intact posterior pole. The enucleation procedure allowed to collect fresh tissues for analysis. Two retinas were taken from donor eyes, obtained within 10 h post mortem. The eyes were sectioned, and the anterior part (including the retina up to the equator) removed; the posterior poles were used for immunohistochemistry on cryosections.

Immunohistochemistry: Human samples were fixed in 4% paraformaldehyde for 24 h at 4 °C and then processed for immunohistochemistry. The samples were rinsed in saline and included in Tissue-Tek® (Sakura, Finetek, Netherlands). For fluorescence immunohistochemistry, 10- μ m-thick neuroretina sections were incubated in blocking buffer (PBS 1X-137 mM, NaCl, 2.7 mM, KCl, 8 mM, Na₂HPO₄, and 2 mM KH₂PO₄, PH 7.4 with 10% fetal calf serum and 0.5% Triton X-100) for 2 h at room temperature, then rinsed in PBS and incubated at 4 °C in primary antibodies listed in Table 2, and diluted in PBS supplemented with 10% fetal calf serum and 0.1% Triton X-100. After washing in the same

TABLE 1. DATA RELATED TO THE OCULAR SAMPLES.

ID	Sex	Age (year)	enucleation	Post mortem (h)	Comments
P1	F	54	+		Peripheral temporal melanoma Normal macula
P2	F	53	+		Peripheral nasal melanoma Normal macula
P3	F	65	+		Ciliary body melanoma Normal macula
P4	F	75		7 h	Normal macula on post mortem observation
P5	M	69		9 h	Kidney failure No ocular history
P6	M	71	+		Ciliary body nasal melanoma Normal macula
P7	M	78	+		Epidermoid carcinoma of the conjunctiva - Normal macula
P8	F	85		34 h	Hypertension. No ocular history - Normal macula

TABLE 2. LIST OF ANTIBODIES USED.

Antibodies	Species	References	Lab provider	Dilution
Anti-GFAP polyclonal central domain of the protein	Rabbit	ZO334	Dako cytotation	1/200
Anti-glutamine synthetase clone GS-6	Mouse	MAB 302	Merck Millipore	1/300
Anti-CRALBP monoclonal	Mouse	MA1-813	Thermo Fisher Scientific	1/300
Anti-vimentin polyclonal	Chicken	Ab24525	Abcam	1/500
Anti-CX43 C-ter domain	Goat	Sc-6560	Santa Cruz	1/200
Anti-ZO1 polyclonal	Rabbit	Sc-10804	Santa Cruz	1/200
Alexa-fluor 488 and 594			Invitrogen	1/300
4',6'-diamino 2-phenylindole DAPI				1/5000

buffer, the sections were incubated with their corresponding secondary antibodies AlexaFluo®488 or AlexaFluo®594 (Invitrogen/Thermo Fisher scientific Carlsbad, CA) for 3 h (Table 2). Sections were counterstained with 4', 6-diamino-2-phenylindole (DAPI, Sigma Aldrich, Saint Quentin Fallavier, France), washed in saline, and mounted in Fluoromount (ThermoFisher Scientific, Herblain, France). Imaging was done with a laser scanning confocal microscope (LSM 710, Carl Zeiss, Munich, Germany) equipped with Zeiss 63x Plan-Apochromat oil immersion objective and the Zeiss ZEN software.

To differentiate the different types of microglial cells in the macula, we used several glial markers, expressed either in astrocytes or in RMG cells. Glial fibrillary acidic protein (GFAP) is expressed in astrocytes and is a marker of astrocytes in the brain and in the retina [12]. GFAP is also faintly expressed in RMG cells, located at the inner part of the RMG cell extension at the ILM. However, GFAP can be overexpressed all along RMG cells in the case of astrogliosis [13,14]. Vimentin is expressed in RMG cells, and not in mature astrocytes [12,15], although it can be expressed in some transformed astrocytes [16]. Glutamine synthetase (GS) is specifically expressed in RMG cells and not in astrocytes [17]. Cellular retinaldehyde-binding protein (CRALBP) is also a marker of RMG cells and is not expressed in astrocytes [18,19]. Connexin 43 is mostly expressed in GFAP-positive astrocytes in the retinal GCL to a lesser extent in the processes of RMG cells [20,21]. To control for nonspecific binding of the secondary antibody, staining was performed with secondary antibodies while omitting the primary antibodies (Appendix 1)

RESULTS

GFAP-positive cells are present at the surface of the foveal pit: Sections of the foveola pit from three patients (P1, P2, and P4) showed the presence of cell nuclei located at the innermost

part of the pit, where only photoreceptor nuclei are present in the outer retina. All other retinal nuclei layers are absent, defining the foveola. The GCL, inner nuclear layer (INL), and outer nuclear layer (ONL) were clearly distinguished at the edges of the foveola. The cells present in the inner layer of the foveola were positively stained by the GFAP antibody, demonstrating their glial origin (Figure 1). These cells had lateral extensions over the retinal surface (Figure 1 insets) and were clearly different from radial central Müller glial cells. Importantly, although present in all the observed specimens, this retinal layer showed inter-individual variability with variable thickness and density.

Glial cells at the roof of the foveal pit express astrocytes but not Müller glial cells markers : To characterize the foveal glial cells, we performed coimmunolocalization of different markers of astrocytes and RMG cells on serial sections. Most of the glial proteins were expressed in the astrocytes and the Müller glia, except GS and CRALBP, which are considered specific RMG cell markers. In the P1 macula, GFAP stained the astrocytes in the nerve fiber layer (NFL) and around the retinal vessels up to the inner plexiform layer (Figure 2A and inset and B). However, GFAP also stained the Z-shaped Müller glial cells (Figure 2B, inset). GS labeled the Müller glial cells as transversal longitudinal cells spanning the entire retina from the INL to the ONL and harboring a Z shape in Henle's fiber layer at the macula (Figure 2C inset and F, and 2D inset). At the foveola, the GFAP-positive cells are not stained by GS (Figure 2E,B,D insets).

In the macula from patient 2 (Figure 3), GFAP stained the foveal inner glial cells and astrocytes around the vessels (Figure 3A,B). Vimentin nicely stained the foveal glial cells at the roof of the pit (called the glial plug) and the RMG cells of the fovea and all along the retina (Figure 3C,D inset). Interestingly, GS also stained the Müller glial cells at the fovea and all along the retina, but did not stain the foveal glial plug (Figure 3E,F inset). Colabeling of glial cells with GFAP and

GS showed that the two markers did not colocalize in the foveal glial plug (Figure 3G, arrow).

The macula of patient 3 (Figure 4) showed two sections of the fovea stained with GFAP (Figure 4A–D and insets) showing GFAP-positive cells around the retinal vessels and GFAP-positive cells in the foveal glial plug (Figure 4A,B inset), which send extensions up to the inner plexiform layer (Figure 4C,D inset). These cells did not extend up to the ONL like the foveal Müller glia (Figure 4I), indicating that two types of glial cells are present at the foveola. Vimentin stained the Müller glial cells and faintly stained the foveal glial plug (Figure 4G,H inset), CRALBP, which is a specific marker for Müller cells, did not stain the foveal glial plug

(Figure 4E,F inset), demonstrating that those cells were not common RMG cells.

The macula of patient 4 (Figure 5) showed GFAP-positive cells at the roof of the foveola pit (Figure 5A,B inset), which sent some extensions toward Henle's fiber layer. CRALBP, which is a specific marker of Müller glial cells, labeled the Z-shaped Müller glia (Figure 5C,D insets) and the foveal Müller glia, but did not stain the foveal glial plug (Figure 5E, arrow).

The macula of patient 5 was folded during the section procedure. Nevertheless, the GFAP and GS colabeling showed again GFAP-positive cells in the foveal pit (Appendix

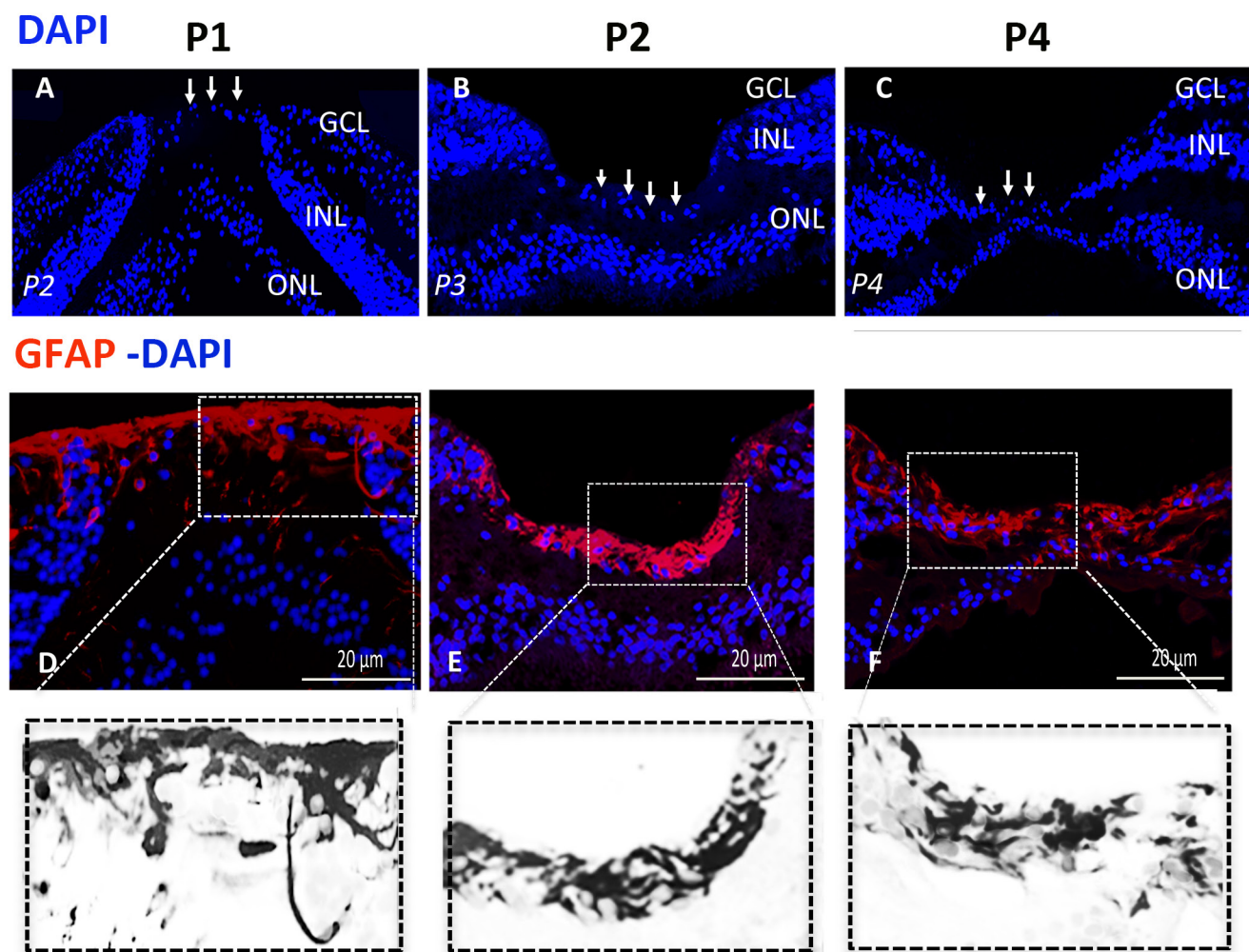


Figure 1. Cryosections and immunolabeling of cells at the roof of the foveal pit. Cryosections (10 µm thick) of the foveola from P1 (A), P2 (B), and P4 (C) showing the presence of cell nuclei (4', 6-diamino-2-phenylindole [DAPI] staining) at the roof of the foveal pit (arrows). Costaining with the glial marker glial fibrillar acidic protein (GFAP) of the foveola from P1 (D), P2 (E), and P4 (F) shows that GFAP-positive cells with lateral extension lie on the roof of the fovea (black and white higher magnification insets). The nuclei of those cells are in the innermost layer and do not send radial extensions toward the outer nuclear layers, demonstrating that these cells are distinct from Müller cone cells. GCL, ganglion cell layer; INL, inner nuclear layer; ONL, outer nuclear layer.

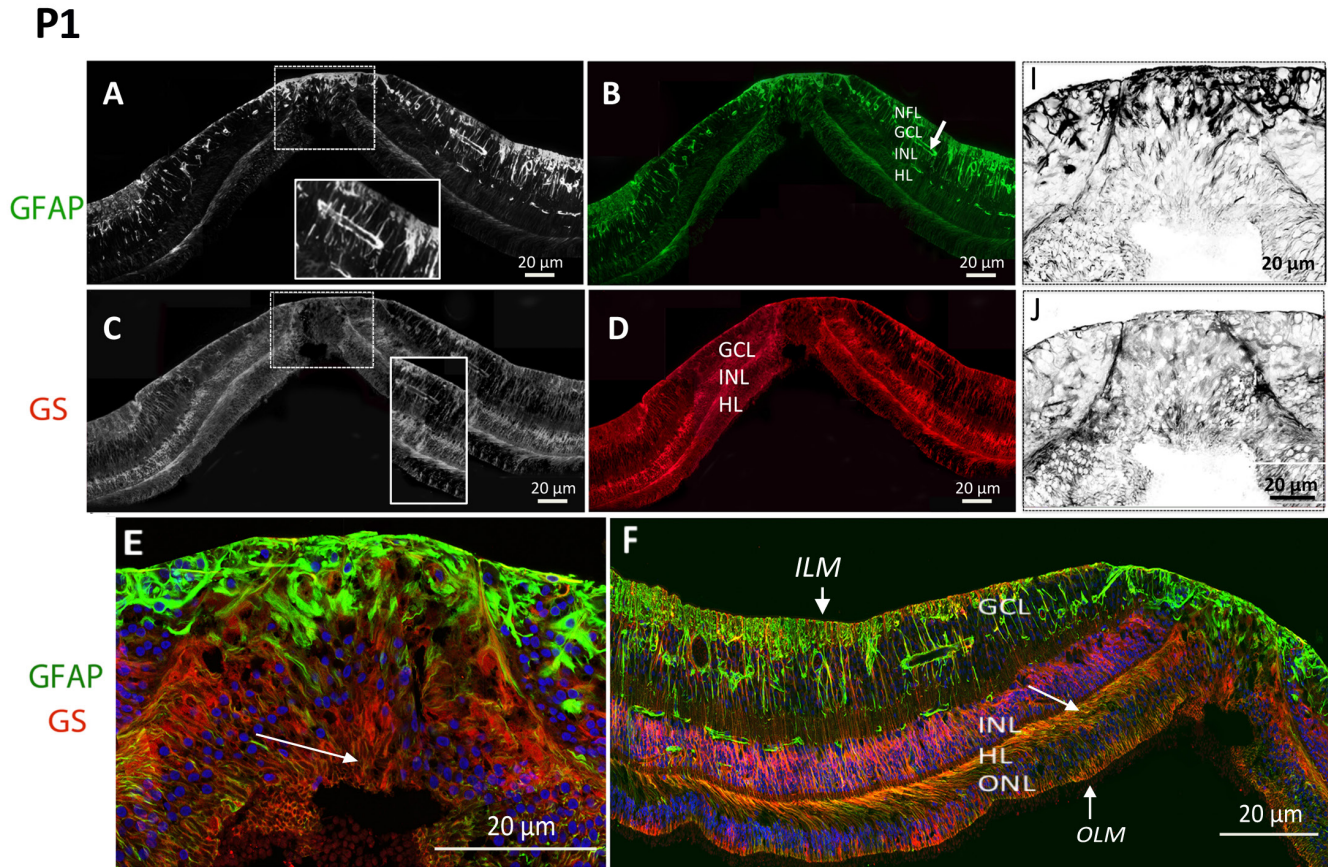


Figure 2. Coimmunostaining of P1 foveal glial cells with the Müller cell marker, GS, and GFAP. Coimmunostaining of foveal cryosections from P1 with glutamine synthetase (GS), which is a specific marker of Müller cells in humans, and with glial fibrillar acidic protein (GFAP) which stains astrocytes and activated retinal Müller glial cells, shows that GFAP-positive cells constitute the roof of the foveal pit **A, B**, and inset) and are not stained with GS (**C, D**, and inset). GFAP stains perivascular astrocytes (**B**, arrow), and GS stains the Müller cells' radial extensions at the fovea (**E**, arrow) and Z-shaped Müller cells in Henle's fiber layer (**F**, arrow). Note that the Z-shaped retinal Müller glial cells also express GFAP (**F**, yellow labeling). GCL, ganglion cell layer; INL, inner nuclear layer; ONL, outer nuclear layer; HL, Henle's fiber layer; OLM, outer limiting membrane.

2 and A inset), and Müller glial cells stained by GS in Henle's fiber's layer and in the fovea (Appendix 2 inset). There was no costaining of the foveola glial plug by the two markers (Appendix 2). In the macula of patient 7, similar GFAP and GS costaining was observed (Appendix 3).

Glial cells at the roof of the foveal pit express Connexin 43: Connexin 43 (Cx43) is the main astrocytic connexin allowing close communication between astrocytes in the brain and in the retina. Cx43 is not specifically expressed in astrocytes, as retinal Müller glial cells have also been shown to express Cx43 in rodents [22] and in humans [20]. In the macula from three patients (P2, P4, and P7), Cx43 was highly expressed in the GFAP-positive foveal cells that formed the roof of the foveola. Cx43 was also expressed faintly in the retinal Müller

glial cells that form Henle's fiber layer, but was not expressed along the foveal cone Müller cells (Figure 6).

DISCUSSION

Using different glial markers, we identified a population of glial cells, resembling astrocytes, that forms the roof of the foveal pit. These cells have a star shape with longitudinal lateral extensions, and their nuclei are located at the innermost part of the foveola. They express astrocyte markers (GFAP, vimentin, and Cx43). We previously showed that they also express aquaporin 4 [23], but they do not express specific markers of Müller glial cells, such as GS and CRALBP, demonstrating that those cells are different from the MCC described by Yamada [8] followed by Gass [9]. Interestingly, in human macula specimens, the nuclei have repeatedly been

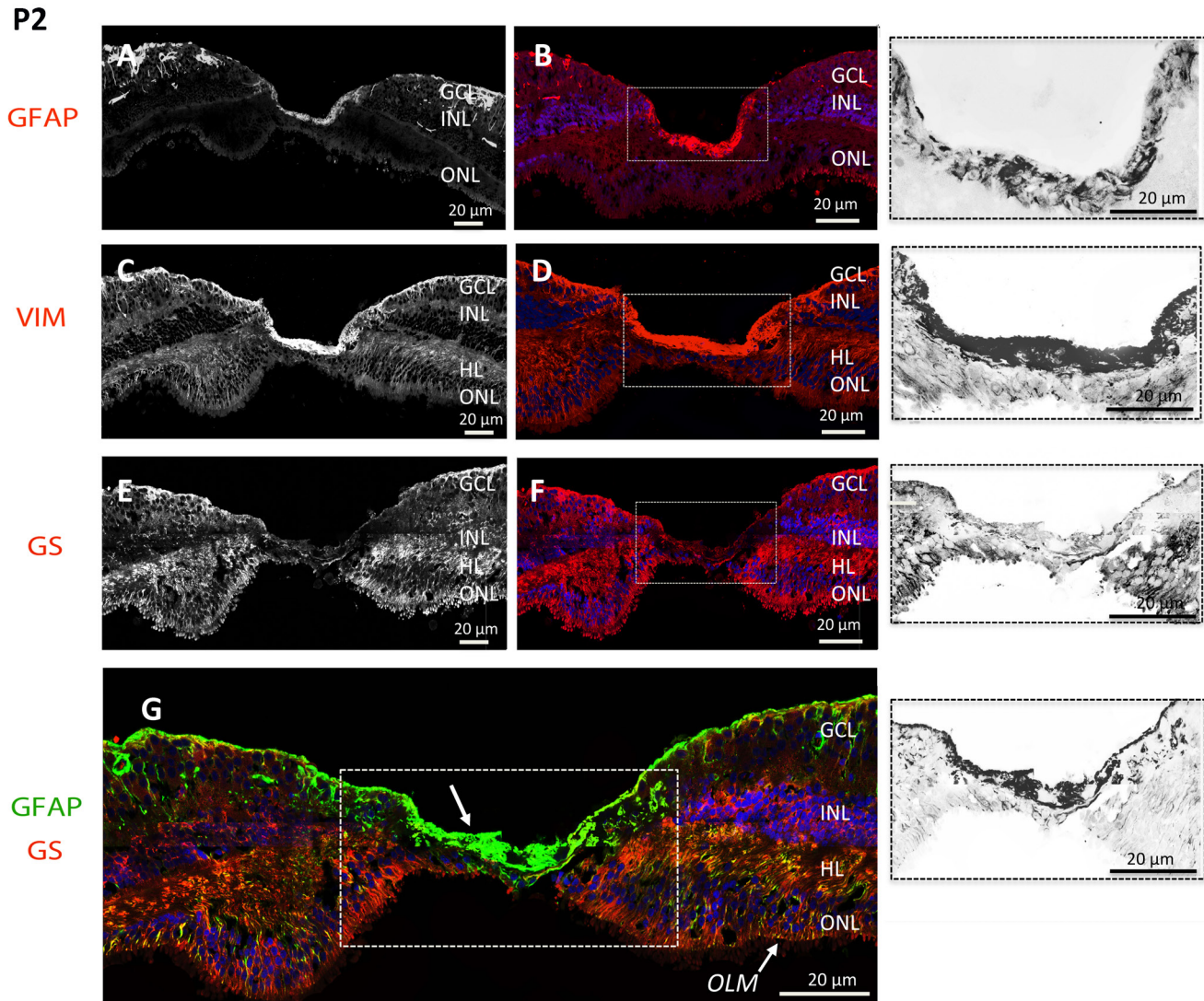


Figure 3. Coimmunostaining of P2 foveal glial cells with the Müller cell marker, GS, GFAP, and vimentin. Coimmunostaining of foveal cryosections from P2 with glutamine synthetase (GS), which is a specific marker of Müller cells in humans, glial fibrillar acidic protein (GFAP), and vimentin (VIM), which stains all glial origin cells, shows that the GFAP-positive cells at the roof of the foveal pit (A, B, and inset) are stained with vimentin (C, D, and inset) but do not express GS (E, F, and inset). Note that vimentin and GS stain the retinal Müller glial cells of the fovea (C, white arrow and inset black arrow) and the Z-shaped Müller cells of Henle's fiber layer (D). GCL, ganglion cell layer; INL, inner nuclear layer; ONL, outer nuclear layer; HL, Henle's fiber layer; OLM, outer limiting membrane.

found at the roof of the foveola, but the type of cells they belong to has never been clarified. Gass hypothesized that these nuclei could be those of the MCC [9], which was not supported by our observations. The presence of astrocytes in the foveola is intriguing. Controversy persists regarding the presence of astrocytes in the central retina before the fovea is formed. Two hypotheses have emerged from studies performed during the development of non-human primate retinas. One hypothesis is that the area where the macula will further develop remains devoid of astrocytes and vessels at all

times [24]. The other is that astrocytes first invade the central retina but then decline prenatally in the perifoveal region [25]. The mechanisms by which the number of astrocytes declines have not been elucidated, as no cell death markers that support the death of astrocytes could be identified during macula development [25]. One of the hypotheses was that foveal astrocytes could lose the expression of GFAP and other glial markers, rather than die, simulating depletion. Thus, foveal astrocytes could be still present in the foveola but be undetectable with classical glial immunolocalization. Interestingly, in

Distler et al.'s study showing a decrease in perifoveal astrocytes, although a clear ring devoid of astrocytes was shown, a subset of stellate astrocytes was still present in the center of the foveola in one adult macaque flatmounted retina, which expressed GFAP [25]. There is still controversy regarding the presence of astrocytes in the fovea. In the present study, we collected adult human maculas from eyes enucleated

because of peripheral malignant tumors and from two human donors with a short postmortem delay (less than 10 h). The fact that we could perform immunohistochemistry on fresh tissues is important as the expression of several glial markers, such as glutamine synthetase can decrease after death. All of the observed samples showed GFAP-positive astrocytes at the roof of the foveal pit, although with interindividual

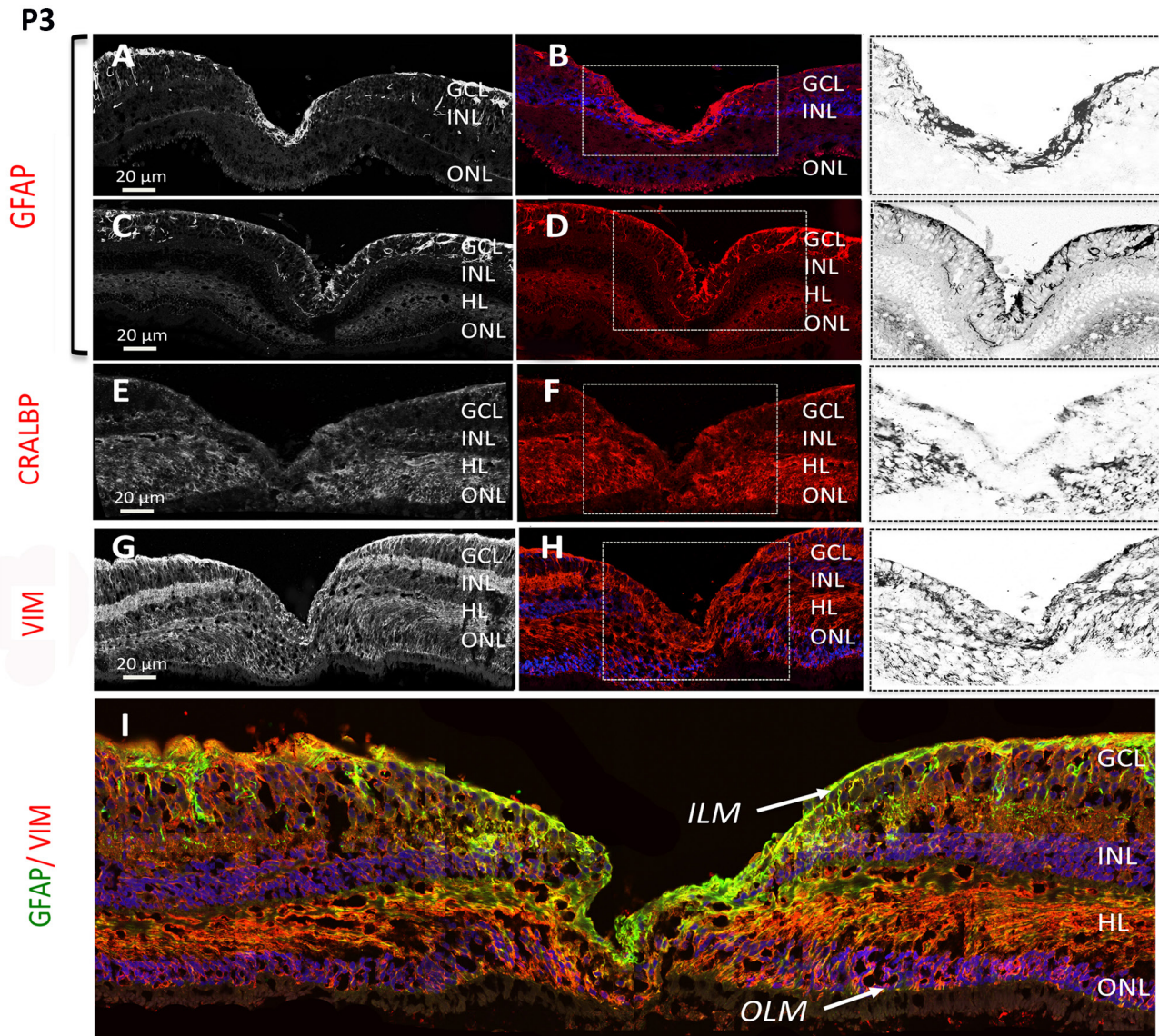


Figure 4. Coimmunostaining of P3 foveal glial cells with the Müller cell marker CRALBP, GFAP, and vimentin. Coimmunostaining of foveal cryosections from P3 with cellular retinaldehyde-binding protein (CRALBP), which is a specific marker of Müller cells in humans, glial fibrillar acidic protein (GFAP), and vimentin (VIM), which stains all glial origin cells, shows that the GFAP-positive cells at the roof of the foveal pit (A, B, C, D, and inset) are stained with vimentin (G, H, and inset) but do not express CRALBP (E, F, and inset). I: Costaining with GFAP and vimentin shows that the GFAP-positive cells at the roof of the pit (arrow) are faintly stained with vimentin and are distinct from the vimentin-positive Müller glial cell extensions (red arrow). GCL, ganglion cell layer; INL, inner nuclear layer; ONL, outer nuclear layer; HL, Henle's fiber layer; OLM, outer limiting membrane.

P4

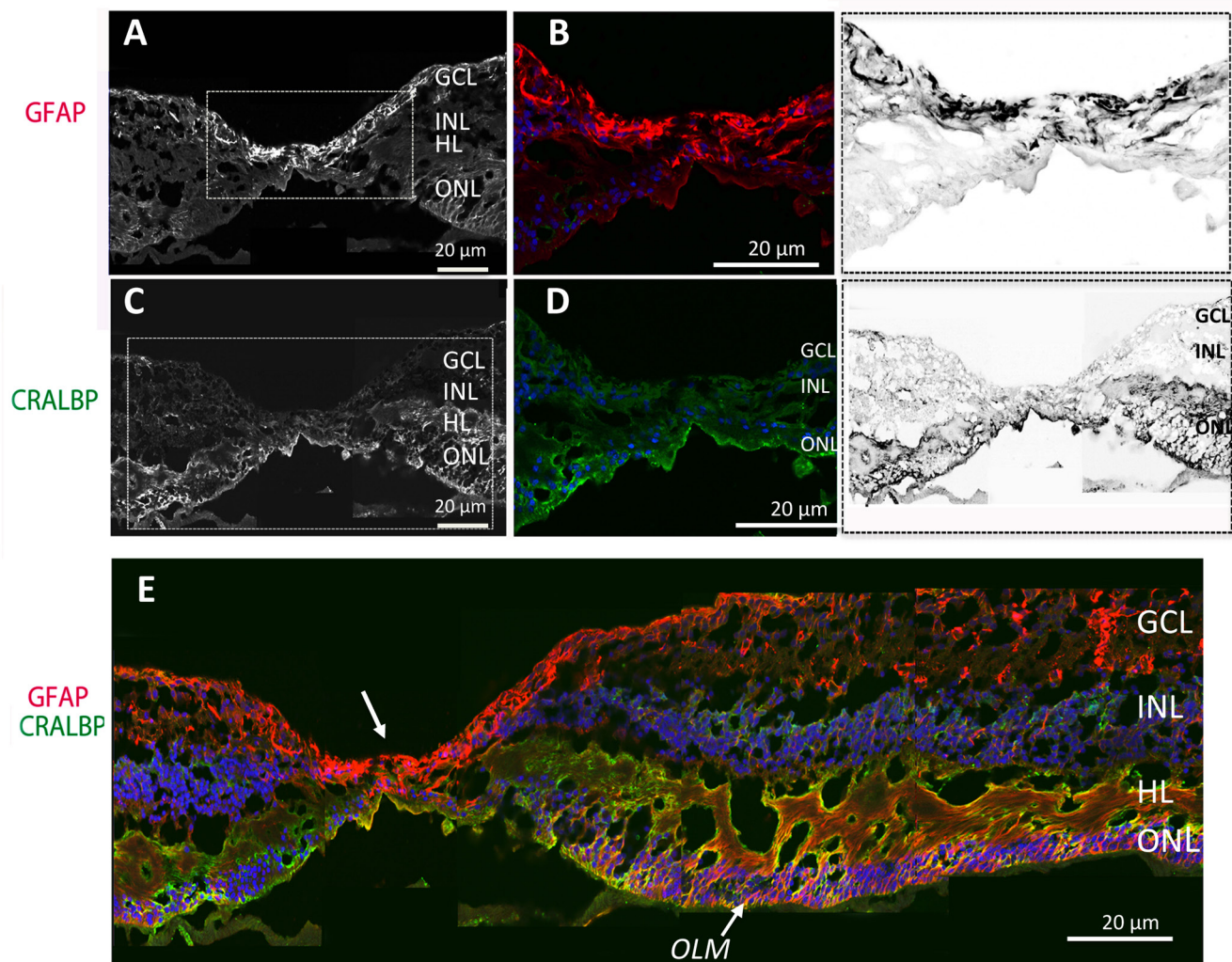


Figure 5. Coimmunostaining of P4 foveal glial cells with the Müller cell marker CRALBP and GFAP. Coimmunostaining of foveal cryosections from P4 with cellular retinaldehyde-binding protein (CRALBP), which is a specific marker of Müller cells in humans, and glial fibrillar acidic protein (GFAP) shows that the GFAP-positive cells at the roof of the foveal pit (A, B, and inset) do not express CRALBP (C, D, and inset). E: Costaining with GFAP and CRALBP shows that the GFAP-positive cells at the roof of the pit (arrow) do not express CRALBP and are distinct from the CRALBP-positive Müller glial cells.

density, indicating that in adult humans, not only MCC but also astrocytes are present in the avascular fovea. To detect this cell population, it is important to perform immunohistochemistry on sections of the posterior segment of the eye, without removing the vitreous, whose traction can induce their detachment, explaining that they might not be detected on flatmounted maculas. As shown in a previous macaque study [24], in the human macula, the glial Z-shaped Müller

cells of the perifoveal region that form Henle's fiber layer express vimentin but also GFAP.

The exact roles of foveal astrocytes have not been determined, but we hypothesize that they could (i) intervene in the foveal pigment import from the vessels to the fovea through the inter-glial communication network, (ii) protect foveal cones from excitotoxicity, (iii) and act as a belt that holds foveal cones and the MCC, in a region where the

inner limiting membrane is the thinnest. This hypothesis is supported by the clinical observation that vitreous traction on the foveal pit can induce the detachment of a dense material during the formation of the lamellar hole, without causing significant functional damage [26] (Appendix 4). If the detached foveal glial cells correspond to the MCC, which is closely linked and attached to cone pedicles, it is unlikely that cones could continue to survive and function normally.

This study has several limitations, such as the limited number of fresh maculas and that some originated from eyes that had a peripheral tumor, which could have induced the

activation of glial cells. However, interestingly, we did not observe in these samples overexpression of GFAP in the retinal Müller glial cells. In addition, the same observation was made on two human donor eyes that were devoid of any known ocular pathology.

In conclusion, this study showed that in the adult human macula, a specific astrocytic cell population covers the roof of the foveal pit. This finding could help understand mechanisms of macular interface pathologies. Further studies are required to determine the origin and roles of this cell population.

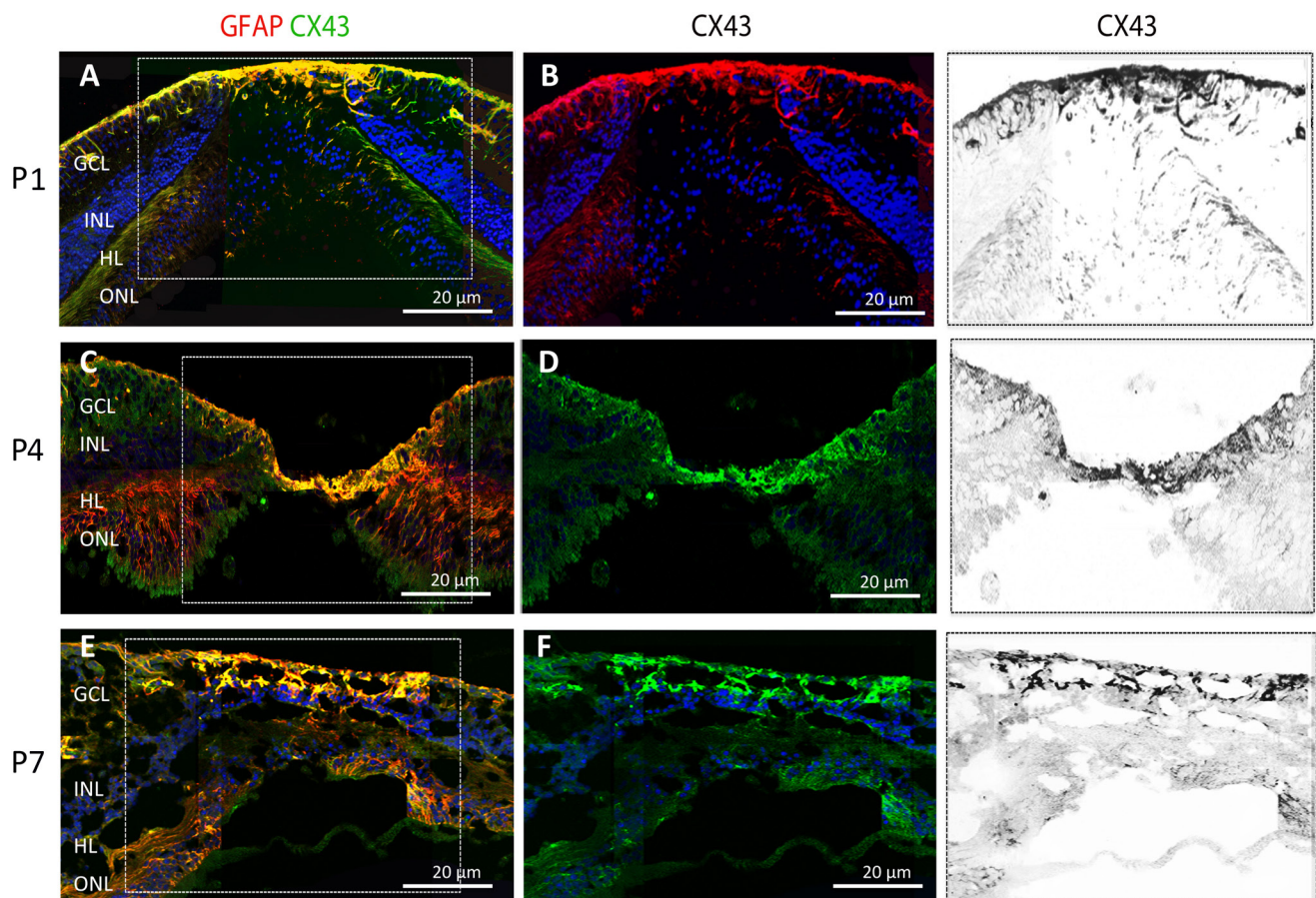


Figure 6. Cx43 and GFAP immunostaining. Glial fibrillar acidic protein (GFAP)-positive astrocytes at the roof of the foveal pit from P1 (A, B, and inset), P4 (C, D, and inset), and P7 (E, F, and inset) express connexin 43 (Cx43). Cx43 is also faintly expressed in retinal Müller glial (RMG) cells in Henle's fiber layer.

APPENDIX 1. TO CONTROL FOR NONSPECIFIC BINDING OF THE SECONDARY ANTIBODY, STAINING WAS PERFORMED WITH SECONDARY ANTIBODIES WHILE OMITTING THE PRIMARY ANTIBODIES.

To access the data, click or select the words “[Appendix 1.](#)” Except from non-specific auto fluorescence of the outer segments, there was no staining with none of the secondary antibodies used in our experiments.

APPENDIX 2. CO-IMMUNOSTAINING OF P5 FOVEAL GLIAL CELLS WITH THE MÜLLER CELL MARKER GLUTAMINE SYNTHETASE (GS) AND GFAP.

To access the data, click or select the words “[Appendix 2.](#)” Co-immunostaining of foveal cryosections from P5 with GS, which is a specific marker of Müller cells in humans and GFAP shows that the GFAP positive cells at the roof of the foveal pit that is folded (A, B and inset) do not express GS (C and D and inset). Co staining with GFAP and GS (E) shows that the GFAP positive cells at the roof of the pit do not express GS and are distinct from the GS positive glial Müller cells, in the fovea and in the Henle layer (E).

APPENDIX 3. CO-IMMUNOSTAINING OF P7 FOVEAL GLIAL CELLS WITH BOTH MÜLLER CELL MARKER GLUTAMINE SYNTHETASE (GS) AND RETINALDEHYDE- BINDING PROTEIN (CRALBP), WITH GFAP.

To access the data, click or select the words “[Appendix 3.](#)” Co-immunostaining of foveal cryosections from P7 with CRALBP and GS, which are specific markers of Müller cells in humans and GFAP shows that the GFAP positive cells at the roof of the foveal pit that is folded (C, E, and F) do not express GS (D and inset) nor CRALBP (B and inset). Co staining of GFAP with CRALBP (E) or GS (F) shows that the GFAP positive cells at the roof of the pit do not express the Müller cell markers that are expressed by cells at the Henle layer.

APPENDIX 4. SD-OCT IMAGES OF MACULAE A.SD-OCT B SCAN OF A WOMAN WHO WAS 75 YEARS OLD, PRESENTING WITH A LAMELLAR HOLE IN FORMATION.

To access the data, click or select the words “[Appendix 4.](#)” The posterior hyaloid remains attached to the dense hyper-reflective roof of the foveal pit, while separation of inner layer occurs at the OPL. B. Five years later, the Henle layer

is stretched and the hyperreflective dense part of the foveola remains on the detached posterior vitreous in front of the foveola (arrow). Note that no epiretinal membrane is detected and that the external limiting membrane and ellipsoid zone are intact. Vision has remained 20/20 during the whole process and the patient has remained asymptomatic.

ACKNOWLEDGMENTS

Centre d'Histologie, d'Imagerie et de Cytométrie (CICC) at Centre de Recherche des Cordeliers, Christophe Klein

REFERENCES

1. Curcio CA, Allen KA. Topography of ganglion cells in human retina. *J Comp Neurol* 1990; 300:5-25. [PMID: 2229487].
2. Curcio CA, Sloan KR, Kalina RE, Hendrickson AE. Human photoreceptor topography. *J Comp Neurol* 1990; 292:497-523. [PMID: 2324310].
3. Burris C, Klug K, Ngo IT, Sterling P, Schein S. How Müller glial cells in macaque fovea coat and isolate the synaptic terminals of cone photoreceptors. *J Comp Neurol* 2002; 453:100-11. [PMID: 12357435].
4. Matet A, Savastano MC, Rispoli M, Bergin C, Moulin A, Crisanti P, Behar-Cohen F, Lumbroso B. En face optical coherence tomography of foveal microstructure in full-thickness macular hole: a model to study perifoveal Müller cells. *Am J Ophthalmol* 2015; 159:1142-1151.e3. [PMID: 25728860].
5. Provis JM, Penfold PL, Cornish EE, Sandercoe TM, Madigan MC. Anatomy and development of the macula: specialisation and the vulnerability to macular degeneration. *Clin Exp Optom* 2005; 88:269-81. [PMID: 16255686].
6. O’Sullivan ML, Puñal VM, Kerstein PC, Brzezinski JA, Glaser T, Wright KM, Kay JN. Astrocytes follow ganglion cell axons to establish an angiogenic template during retinal development. *Glia* 2017; 65:1697-716. [PMID: 28722174].
7. Gariano RF, Sage EH, Kaplan HJ, Hendrickson AE. Development of astrocytes and their relation to blood vessels in fetal monkey retina. *Invest Ophthalmol Vis Sci* 1996; 37:2367-75. [PMID: 8933753].
8. Yamada E. Some structural features of the fovea centralis in the human retina. *Arch. Ophthalmol. Chic. III* 1969; 1960:151-9. [PMID: 4183671].
9. Gass JD. Müller cell cone, an overlooked part of the anatomy of the fovea centralis: hypotheses concerning its role in the pathogenesis of macular hole and foveomacular retinoschisis. *Arch. Ophthalmol. Chic. III* 1999; 1960:821-3. [PMID: 10369597].
10. Govetto A, Bhavsar KV, Virgili G, Gerber MJ, Freund KB, Curcio CA, Burgoyne CF, Hubschman J-P, Sarraf D. Tractional Abnormalities of the Central Foveal Bouquet in Epiretinal Membranes: Clinical Spectrum and Pathophysiological

- Perspectives. *Am J Ophthalmol* 2017; 184:167-80. [PMID: 29106913].
11. Ikeda T, Nakamura K, Oku H, Horie T, Kida T, Takai S. Immunohistological Study of Monkey Foveal Retina. *Sci Rep* 2019; 9:5258-[PMID: 30918305].
 12. Tao C, Zhang X. Development of astrocytes in the vertebrate eye. *Dev. Dyn. Off. Publ. Am. Assoc. Anat.* 2014; 243:1501-10. [PMID: 25236977].
 13. Bringmann A, Pannicke T, Grosche J, Francke M, Wiedemann P, Skatchkov SN, Osborne NN, Reichenbach A. Müller cells in the healthy and diseased retina. *Prog Retin Eye Res* 2006; 25:397-424. [PMID: 16839797].
 14. Bringmann A, Wiedemann P. Müller glial cells in retinal disease. *Ophthalmol. J. Int. Ophthalmol. Int. J. Ophthalmol. Z. Augenheilkd.* 2012; 227:1-19. [PMID: 21921569].
 15. Chu Y, Hughes S, Chan-Ling T. Differentiation and migration of astrocyte precursor cells and astrocytes in human fetal retina: relevance to optic nerve coloboma. *FASEB J. Off. Publ. Fed. Am. Soc. Exp. Biol.* 2001; 15:2013-5. [PMID: 11511521].
 16. Pérez-Alvarez MJ, Isiegas C, Santano C, Salazar JJ, Ramírez AI, Triviño A, Ramírez JM, Albar JP, de la Rosa EJ, Prada C. Vimentin isoform expression in the human retina characterized with the monoclonal antibody 3CB2. *J Neurosci Res* 2008; 86:1871-83. [PMID: 18241054].
 17. Bringmann A, Pannicke T, Biedermann B, Francke M, Iandiev I, Grosche J, Wiedemann P, Albrecht J, Reichenbach A. Role of retinal glial cells in neurotransmitter uptake and metabolism. *Neurochem Int* 2009; 54:143-60. [PMID: 19114072].
 18. Bunt-Milam AH, Saari JC, Klock IB, Garwin GG. Zonulae adherentes pore size in the external limiting membrane of the rabbit retina. *Invest Ophthalmol Vis Sci* 1985; 26:1377-80. [PMID: 4044165].
 19. Kennedy BN, Li C, Ortego J, Coca-Prados M, Sarthy VP, Crabb JW. CRALBP transcriptional regulation in ciliary epithelial, retinal Müller and retinal pigment epithelial cells. *Exp Eye Res* 2003; 76:257-60. [PMID: 12565814].
 20. Danesh-Meyer HV, Zhang J, Acosta ML, Rupenthal ID, Green CR. Connexin43 in retinal injury and disease. *Prog Retin Eye Res* 2016; 51:41-68. [PMID: 26432657].
 21. Kerr NM, Johnson CS, de Souza CF, Chee K-S, Good WR, Green CR, Danesh-Meyer HV. Immunolocalization of gap junction protein connexin43 (GJA1) in the human retina and optic nerve. *Invest Ophthalmol Vis Sci* 2010; 51:4028-34. [PMID: 20375327].
 22. Theofilas P, Steinhäuser C, Theis M, Derouiche A. Morphological study of a connexin 43-GFP reporter mouse highlights glial heterogeneity, amacrine cells, and olfactory ensheathing cells. *J Neurosci Res* 2017; 95:2182-94. [PMID: 28370142].
 23. Daruich A, Matet A, Moulin A, Kowalczyk L, Nicolas M, Sellam A, Rothschild P-R, Omri S, Gélizé E, Jonet L, Delaunay K, De Kozak Y, Berdugo M, Zhao M, Crisanti P, Behar-Cohen F. Mechanisms of macular edema: Beyond the surface. *Prog Retin Eye Res* 2018; 63:20-68. [PMID: 29126927].
 24. Provis JM, Sandercoe T, Hendrickson AE. Astrocytes and blood vessels define the foveal rim during primate retinal development. *Invest Ophthalmol Vis Sci* 2000; 41:2827-36. [PMID: 10967034].
 25. Distler C, Kopatz K, Telkes I. Developmental changes in astrocyte density in the macaque perifoveal region. *Eur J Neurosci* 2000; 12:1331-41. [PMID: 10762362].
 26. Frisina R, Pilotto E, Midena E. Lamellar Macular Hole: State of the Art. *Ophthalmic Res* 2019; 61:73-82. [PMID: 30625477].

Articles are provided courtesy of Emory University and the Zhongshan Ophthalmic Center, Sun Yat-sen University, P.R. China. The print version of this article was created on 1 April 2020. This reflects all typographical corrections and errata to the article through that date. Details of any changes may be found in the online version of the article.